Allometric Relationships of Selected European Tree Species

Parametrizations of tree architecture for the purpose of 3-D canopy reflectance models used in the interpretation of remote sensing data

Betula pubescens, Fagus sylvatica, Larix decidua, Picea abies, Pinus sylvestris

EUROPEAN COMMISSION
JOINT RESEARCH CENTRE

2003

Institute for Environment and Sustainability

EUR 20855 EN

Allometric Relationships of Selected European Tree Species

Parametrizations of tree architecture for the purpose of 3-D canopy reflectance models used in the interpretation of remote sensing data.

Betula pubescens, Fagus sylvatica, Larix decidua, Picea abies, Pinus sylvestris

Jean-Luc Widlowski
Michel Verstraete
Bernard Pinty
Nadine Gobron

EC Joint Research Centre, TP 440
I–21020 Ispra (VA), Italy

EUROPEAN COMMISSION
JOINT RESEARCH CENTRE

2003

ies
Institute for Environment and Sustainability

EUR 20855 EN

A great deal of additional information on the
European Union is available on the Internet.
It can be accessed through the Europa server
(http://europa.eu.int)

EUR 20855 EN

Printed in Italy

Contents

Executive Summary

This document presents a selection of allometric equations describing tree architectural properties — like the tree height, crown dimensions, leaf area index and biomass — for the following tree species: European beech (*Fagus Sylvatica*), birch (*Betula pendula* and *Betula pubescens*), European larch (*Larix decidua*), Norway spruce (*Picea Abies*) and Scots pine (*Pinus sylvestris*). The purpose of this collection of allometric relationships is to facilitate the generation of statistically correct, three-dimensional forest architecture representations for inclusion in 3-D radiation transfer simulations. At the time of writing, no single document was available that facilitated such a task for these tree species.

1 Introduction

The purpose of this document is to compile information from the published literature to permit a statistically faithful reconstruction of the structural characteristics of selected European tree species over areas that are comparable to the instantaneous field of view (IFOV) of most current medium spatial resolution instruments (50 - 500 m). Such spatially and structurally explicit information is required by the latest generation of 3-D radiation transfer models in order to simulate the bi-directional reflectance fields of credible forest scenarios for their later perusal in the interpretation process of satellite based observation of the Earth's surface.

1.1 Background

About 3.9 billion hectares or 30% of the Earth's surface are covered by forests, of which 33% are located in the boreal and 11% in the temperate ecological zones. The European Union is currently home to about 87 million hectares of forest, ranking it the 8^{th} largest forest area in the world after Russia, Brazil, Canada, the United-States, China, the democratic republic of Congo, and Indonesia. However, with the accession of the Central and Eastern European countries this number may even rise to 140 million hectares. Impartial, accurate and up-to-date information as regards the state, health and development of the European forests is thus needed—not only because of their recreational value for the citizen—but because their presence, age and structural properties affect 1) the exchanges of water, carbon and trace gases between the the vegetation canopy and the atmosphere, 2) the degree of soil erosion and desertification, 3) the local input to the global carbon cycle whose processes, although not entirely understood, require the presence of a terrestrial carbon sink component in order to balance the overal budget, 4) the amount of available woody biomass which is the raw material for a global multi-billion dollar timber industry, and 5) the population dynamics and biodiversity of animals, insects and birds they host. Furthermore, with the ratification of the Kyoto Protocol, the accurate biomass estimation of existing forest resources is an integral component of the carbon trading process, that allows industrialized nations to actively promote certain kinds of carbon sinks through forest plantations in order to meet their greenhouse gas emissions reduction commitments.

Assessing the structural properties of individual trees, even for a moderate forest area is a major endeavour. For example, there are about 65 billion trees higher than 1.3 m in Finland (Tomppo 2000). Rather than measuring every single tree, forest inventories are designed to provide reliable estimates of timber volume, growth, removals, and mortality on the basis of sampling schemes that have been perfected by the commercial sector in order to derive sufficiently accurate properties of tree populations at minimal cost. The chief drawbacks of forest inventories are that the inventory practices vary widely among countries, and so do the uncertainties. Since inventories are expensive and time consuming, they are typically conducted only once every five to ten years, depending on the type (and scale) of the inventory. In large countries such as Canada and Russia, some remote regions are not sampled at all. Most inventories are rolling in nature, that is, not all regions in a country are sampled at the same time; and successive inventories in some cases tend to be updates and/or revisions, and thus are not necessarily time series data. To alleviate these issues, satellite image-based inventories have been applied as early as the 1990s by some European countries. This is because space-borne remote sensing techniques have the conceptual advantages of acquiring quantitative data over large areas in a relatively short period of time, and this at a fixed spatial resolution and on a regular basis. The widespread use of these technologies has, however, been hampered in the past, due to the lack of 1) validated 3-D radiation transfer models (and procedures) suitable for inversion purposes, 2) sufficiently fast computer hardware for (quasi-)operational processing,

and 3) well-calibrated, high spatial resolution, multi-spectral data befitting the quantitative extraction of surface parameters needed in forest inventories.

This situation is however likely to improve through advances in space technology and in a better understanding of the radiation transfer processes within vegetation canopies, which allows us to develop and advance the capabilities of models to simulate these processes. For example, nowadays it is known that when the spatial resolution of the sensor becomes of the same order of magnitude as the size of the trees, the extraction of quantitative surface structure information from remote sensing measurements requires taking into account the details of the structure and heterogeneity of the canopy. This is best achieved using three dimensional (3-D) radiation transfer (RT) models, that are nowadays capable of representing the relevant radiation transfer processes within heterogeneous environments of almost any degree of complexity (subject to computer memory), *e.g.*, Govaerts (1996), Thompson and Goel (1998), North (1996). Since the goal of remote sensing is the retrieval of one or more state variables describing the system under observation, radiation transfer models have to be inverted against the gathered data to achieve this. However, given the large number of variables in the above 3-D models, it is desirable to narrow the solution space of such inversions by excluding all unlikely surface type candidates from the start. By the same token, one can predefine all surface structure solutions that are likely to be encountered, compute their bi-directional reflectance patterns and store these values in a so called look-up-table (LUT) for later perusal in the actual inversion process against the satellite-measured data strings. The goal in these approaches is to identify the "most likely" candidate from amongst the set of pre-defined 3-D surface type solutions (in the LUT) that satisfies the space-borne reflectance observations within some documented range of accuracy. Previous applications of such LUT-based inversion schemes were restricted by their region/biome of interest, the number/simplicity of potential surface type candidates in the LUT, and the available (coarse spatial resolution, multi-spectral but mono-directional) optical remote sensing measurements, *e.g.*, Govaerts et al. 1997, Myneni et al. 1997, Knyazikhin et al. 1998, Widlowski et al. 2001. Given the impact of 3-D surface structures on the bi-directional reflectance signature of terrestrial targets (Pinty et al. 2002) and the recent availability of well calibrated, narrow spectral band sensors with a high signal-to-noise ratio—such as the Multi-Angle Imaging SpectroRadiometer (MISR) on board Terra (Diner et al. 1998)—a more detailed surface structure characterisation is required if 3-D LUT based inversion techniques are to satisfy the needs of the scientific community for enhanced surface structure information.

One of the main drawbacks of LUT-based inversion approaches is the multiplicity of retrieved solutions, especially for mono-directional, low spatial resolution spaceborne instruments. This can however, be alleviated by quasi-instantaneous multi-directional and multi-spectral sensors at sufficiently high spatial resolutions, like MISR, to constrain the solution space for the retrievals. At the finer spatial resolutions, the surface structure contained within and around the instantaneous field of view (IFOV) of the observing sensor is of increasing relevance with respect to the angular shape of the reflectance anisotropy. Thus, in the context of LUT based inversion schemes it is crucial to know the relevant structural (and to a similar degree also spectral) properties of the canopy with sufficient detail and accuracy to allow for the simulation of bidirectional reflectance fields. Such information would not only reduce the number of surface type candidates that will have to be included in a 3-D LUT based inversion scheme, but also guarantee that the structural and spectral characteristics of any "most likely" surface type candidate have actually been measured (at least once) on real specimens, either in the field or laboratory. Once such a "most likely" surface type candidate has been determined in a temporally stable manner, all sorts of statistics can be performed at the within-pixel level since all structural and spectral details related to its construction are known.

1.2 Purpose and scope

The purpose of this document is thus to compile allometric relationships, that are based on field observations and that describe the structural properties of an individual tree, for the subsequent generation of credible surface structure solutions (forest canopies) over spatial scales that are comparable to the IFOV of most current medium spatial resolution instruments. From a radiative point of view (as well as computer memory considerations) it is thus not necessary (or feasible) to represent every single leaf/needle within the nominal IFOV area, but rather to ascertain that the faithful reconstruction of these architectural characteristics is guaranteed in a statistical manner within the area of interest, say 100×100 m^2 or larger. The primary focus of this document thus pertains to the structural characteristics of an individual tree. Estimates of tree height, crown length, -width, -shape and amount of foliage that are contained there within will be provided. Obviously some degree of abstraction is inevitable, especially when dealing with the shape of tree crowns. We provide examples of crown shape approximation through the usage of two or more geometrical primitives (cones, cylinders, etc). However, other more complex crown representations might be appropriate, *e.g.*, Kranigk et al. (1994). As regards the orientation and distribution patterns of foliage elements within the tree crowns, only limited species-specific information is available. The same applied to species mixtures, dead wood percentages, phenological variations of leaf area and the recession of crown dimensions with increasing tree density. Some of these topics, together with the spatial distribution patterns of trees, will thus be dealt with in a special section at the end of this document.

While every effort has been made to retain the allometric relationships and measurements as they were published in the literature, in some instances these studies aimed primarily at fitting their available data rather than providing an equation that covered the entire known range of the controlling variable (usually the diameter at breast height, DBH). Thus, in order to obtain meaningful results over as broad as possible range of tree sizes, an empirical curve-fitting occasionally had to be applied to an existing allometric relationship such as to allow for a reasonable behaviour at very low and high values of the controlling variable *i.e.*, as the DBH approaches zero or very large values.

All the information used to generate this document is freely accessible from the Internet or through the published literature. However, many of these documents were not useful for the purpose of this compilation because the information contained there was 1) too complex, in the sense that it required the knowledge of a large number of parameters not generally available to the modeller, 2) too general, in the sense that it related to spatial scales (stand or forest) much greater than that of the individual tree, or 3) incomplete, in the sense that (from a modelling point of view) some of the crucial variables were missing. Consequently, this document does not claim to be complete or exhaustive. In fact, given the large latitudinal range of some of the species described below, and the many possible combinations of soil types, species mixtures, stem densities, and other stress factors that affect the growth and productivity of trees (not to mention the meteorological variability occurring from year to year), the reader will still need to decide which of the provided allometric equations best fits his needs and requirements.

1.3 Variables and definitions

A variety of structural variables have to be known to generate three-dimensional forest canopy representations in the context of radiation transfer simulations. For example, the 'crown shape' and 'foliage content' affect the amount and angular distribution of the reflected radiation; 'tree height' together with the density and spatial distribution of the trees determine both the crown dimensions and foliage content, as well as the angular width of reflectance peak close to the

retro-reflection direction. In traditional forestry most structural properties, like tree height, crown width, crown length, etc, have been related by allometric relationships to an easily measurable primary variable. In most cases this variable is the Diameter-at-Breast-Height, DBH, *i.e.*, the diameter of the tree trunk at a height of 1.37 m above the ground. The DBH parameter is commonly expressed in units of centimetres [cm], whereas most of the allometrically derived quantities (in Europe) retain their SI units, *i.e.*, they are expressed in units of metres [m].

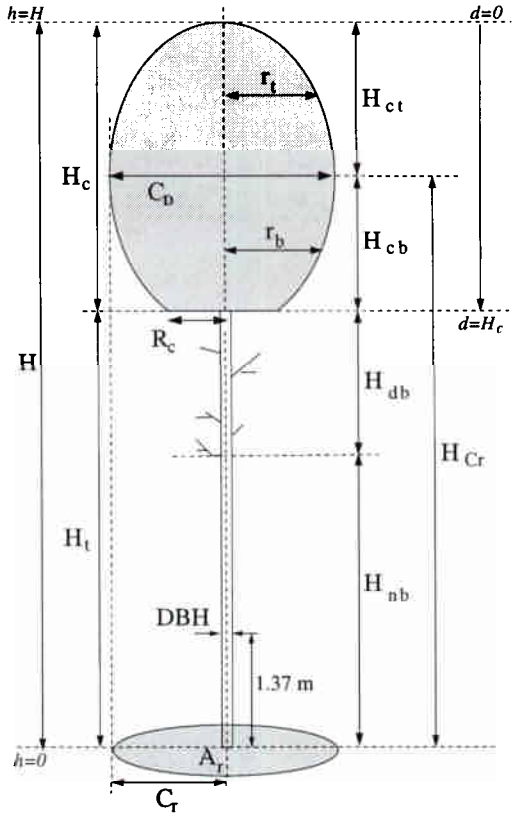

Figure 1: Schematic tree with 'tree height' (H) being the sum of the total 'crown length' (H_c) and the 'ground to crown' distance (H_t), where the crown length is composed of an (illuminated) 'crown top' (H_{ct}) and a (shadowed) 'crown bottom' (H_{cb}) distance. The crown partitioning lies at a height where the maximum crown diameter (C_D) occurs. Similarly the 'ground to crown' length (H_t) can be subdivided into a 'height to first dead branch' (H_{nb}) and a length describing the height regime where 'dead branches' (but no foliage) occur along the tree trunk (H_{db}). The crown radius at the 'bottom of the crown' (R_c) as well as the vertically downward projected crown area (A_l) are also indicated.

Underlying the generation of any forest canopy scene is either a distribution of DBH values from which the corresponding tree height distribution can be derived, or, vice versa, a tree-height distribution from which the DBH values can be retrieved by inverting the appropriate allometric relationship for that tree species. Within this document, the overall **tree height**, H is always the sum of the total crown length (H_c) and the **ground to crown** length (H_t), where the crown length is composed of a (sunny) top part (H_{ct}) and a (shady) bottom part (H_{cb}). Similarly, the ground-to-crown length can be subdivided into a **height to the first dead branch** (H_{nb}) and a length describing the height regime where dead branches (but no foliage) occur along the tree trunk (H_{db}). Alternatively the **height to the maximum crown width**, H_{Cr} indicates the vertical distance to the interface between the illuminated and shadowed crown halves. Hence:

$$H = H_c + H_t = (H_{ct} + H_{cb}) + (H_{db} + H_{nb}) = H_{ct} + H_{Cr} \quad [\mathrm{m}]$$

For the purpose of modelling large ensembles of tree crowns, the latter volumetric entities have to be abstracted to allow for a computer efficient representation of their outer envelope, as well as, their wood and foliage content. Where available, **crown shape** approximations similar to those of Pretzsch (1992) will be given. Such representations use two (or more) geometrical primitives (cone, hemisphere, cylinder) whose bases meet at the interface between the sunny (top) and shady (bottom) portions of the crown. As such their largest lateral expansion can be used as a measure of the **maximum crown radius**, C_r [m]. Depending on the shape of the crown, an estimate of the **bottom crown radius**, R_c [m] is also required to model the geometric representations of the crown. Where available, the change of the crown radius in both the top part (r_t) of the crown (for distances $0 < d \leq H_{ct}$) and the bottom part (r_b) of the crown (for distances $H_{ct} < d \leq H_c$) may be expressed in terms of the distance from the the top of the tree (d) as described by Pretzsch (1992). However, trees are very complex entities and the geometric crown shape models are rather abstract representations of reality, which has prompted many scientists to look for more appropriate descriptions of tree architecture, ranging from asymmetric ellipsoids to explicit L-system representations, *e.g.*, Cescatti (1997), De Reffye and Houllier (1997) and Goel et al. (1991).

The **needle/Leaf Area Index**, LAI [m^2/m^2] is a particularly critical value in the context of radiation transfer simulations since it is through their foliage elements that plants absorb (predominantly at the shorter end of the solar spectrum, *i.e.*, 350 - 700 nm) and reflect (mostly in the near-infrared part of the optical domain, *i.e.*, 700 - 2500 nm) the incoming radiation. The meaning of LAI that is used within this document relates to the ratio of the 'one sided area of foliage elements of a single tree' and the 'vertically projected crown area of that tree'. Accurate LAI estimates are however rare, with large differences between estimates for specific biomes (Scherzer et al. (2003) for example, report that LAI values for coniferous forests have been estimated in the scientific literature to lie between 6 and 10). Temporal variations of LAI (due to the phenology) are even less often available. In this document LAI estimates are given as provided by their authors, citing as much additional information as was available on the stand characteristics of their study. In some cases, however, the LAI value has to be derived from independent studies of leaf area A_l and downward projected crown area (A_r), which in the case of the radially symmetric crown model of Pretzsch (1992) reduces to the cross-sectional area of the tree crown at its maximum lateral extent, *i.e.*, $A_r = \pi C_r^2$. It should be kept in mind, however, that an LAI definition *per individual tree* is different from the stand projected LAI often found in the literature, since the latter depends both on the stem density and height of the trees in the plot (as well as the understory cover). Last but not least, information on the **foliage and biomass** characteristics are also provided for every tree species.

1.4 Document structure

The document is subdivided into two sections. The first section lists species-specific allometric relationships for the deciduous tree species: Beech *(Fagus sylvatica)* and birch *(Betula pubescens* and *Betula pendula)*, as well as for the coniferous tree species: larch *(Larix decidua)*, Norway spruce *(Picea abies)*, and Scots pine *(Pinus sylvestris)*. These tree species were identified because they represent a large fraction of the available forest resources in Europe, especially in northern latitudes where Scots Pine and Norway Spruce dominate the landscapes, but also within central and eastern Europe. In addition, a variety of birch species exist throughout the Northern hemisphere, and larch is a widely occurring tree species within Russia *(Larix siberica)*. For each of these tree types—and the previously identified structural parameters—a series of allometric relationships will be provided, together with a graphical representations of these

functions. Equations that are contained in a framed box are those that have been implemented by the Science and Technology for Applied Remote Sensing ($\mathcal{STARS}$) group to generate three-dimensional forest scenes for later processing using the 3-D radiation transfer model of Govaerts and Verstraete (1998). The second section of this document describes canopy characteristics for which either not enough species-specific information was available, or, cases where these properties were not species-dependent. The document closes with a list of symbols and a list of reference materials that were used in its generation.

1.5 Feedback

This document aims at providing credible allometric relationships for the three-dimensional reconstructions of tree-like entities in the context of 3-D radiation transfer simulations. To this effect, a series of (somewhat abstracted) structural properties of a series of selected tree species are presented. A higher degree of realism has not been adopted because of the difficulties in finding further structurally relevant information, *e.g.*, branching patterns and angles, foliage orientation changes along the vertical gradient of the crown, seasonal LAI variations, crown adaptations to competition, etc. Nevertheless, the structural variables that are described within this document can be considered sufficient for the simulation of radiation transfer processes within vegetation canopies covering areas equivalent to the IFOV of at medium to high spatial resolution sensors. To carry out such radiation transfer simulations requires, however, not only information regarding the structural properties of the vegetation, but also spectral information describing their reflective and absorptive characteristics. Some possible sources for soil and foliage spectra may be found at the JRC Leaf Optical Properties Experiment (LOPEX'93) web site: `http://www.sigu7.jussieu.fr/Led/LED_lopex.htm` or at the Jet Propulsion Laboratory spectral library web site: `http://speclib.jpl.nasa.gov`. The authors' experience is that foliage reflectance spectra are relatively abundant, whereas bark reflectance and also leaf transmission spectra are rather difficult to obtain, especially when aiming at discriminating between these properties for the upper and lower leaf sides separately. Even more difficult to locate are descriptions of the angular reflectance probabilities of such surfaces, *i.e.*, the bi-directional reflectance distribution function (BRDF). In most radiation transfer simulations, scatterers are thus modelled as isotropic surfaces.

Any constructive comments with respect to the information contained in this document, as well as additional input regarding new or already described structural and spectral properties is welcome and should be addressed to *Jean-Luc.Widlowski@jrc.it*. They may be incorporated in updated or future reports of this kind.

Allometric Relationships of Selected Tree Species

The first part of this document provides allometric relationships to describe the structural attributes of the following tree species: Birch *(Betula pendula* and *Betula pubescens)*, European beech *(Fagus sylvatica)*, European larch *(Larix decidua)*, Norway spruce *(Picea abies)*, and Scots pine *(Pinus sylvestris)*.

2 Birch (*Betula pubescens* and *Betula pendula*)

The two major European birch species (*Betula pubescens* and *Betula pendula*) are naturally occurring throughout Europe. *Betula pendula* tends to be larger and wider than *Betula pubescens*, and does not occur far into the northern latitudes as the latter. Conversely, *Betula pubescens* does hardly occur in southern Europe, but can be found in central Europe and in the northern boreal zone, and this throughout Europe and Russia. Even in Greenland *Betula pubescens* can reach heights of up to 2.5 m (Röhrig 1980). Birch trees tend to occupy flat or slightly undulating lowlands. Nevertheless, they can also be found up to elevations of about 1000 m (or up to 1800 m in the Alps).

2.1 Crown shape

Birch trees are relatively exigent as regards the availability of light. They are resistant against cold/frost and thus often act as pioneer trees that occupy empty tracts of land. However, due to their need for large amounts of light, as well as, their short-livedness they tend to get replaced by other tree species. *Betula pubescens* is often encountered on wet soils. The bark is whitish, grey or silvery with black fissures appearing at the base of the trunk. The crown shape of the birch can be represented using an obloid (whose major axis is of length H_{ct} and whose radial axis is of size C_r) and a hemisphere that are connected by a cylinder, which represents the widest part of the vertically elongated crown, as indicated in the middle graph of Figure 2. The right hand panel in the same Figure shows a 3-D visualization of a mature birch stand with a somewhat more differentiated crown shape representation.

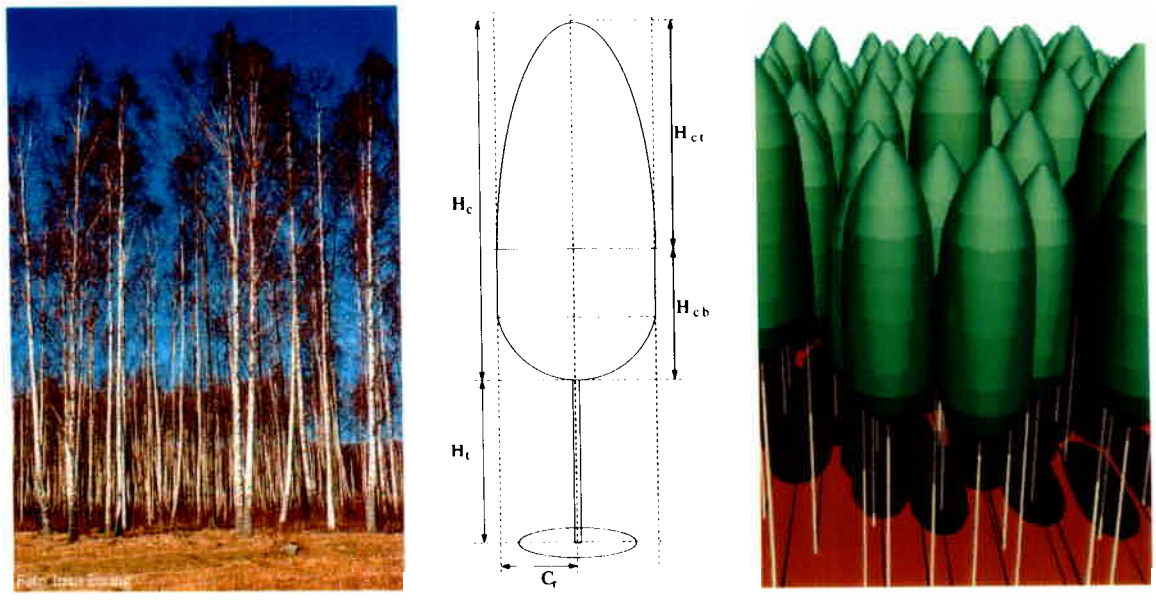

Figure 2: Left panel: *Betula pubescens* tree photographed by Anna-Lena Anderberg, (Source: `http://linnaeus.nrm.se/flora/`). Middle panel:Crown model of *Betula pubescens*. Right Panel: 3-D visualization of a 20 m high birch stand for which the reflectance fields can be modelled using the radiation transfer model of Govaerts and Vertstraete, 1998.

2.2 Tree height, H [m]

The JABOWA model of Botkin (1993) provides tree height equations for a series of Betula species, *i.e.*, yellow birch *Betula alleghaniensis*, white or paper birch *Betula papyrifera* and gray birch *Betula populifolia*.

$$
\begin{aligned}
H &= 1.37 + 0.583\,DBH - 0.00291\,DBH^2 \quad [\text{m}] \quad \textit{Betula alleghaniensis} \\
H &= 1.37 + 0.766\,DBH - 0.00504\,DBH^2 \quad [\text{m}] \quad \textit{Betula papyrifera} \\
H &= 1.37 + 0.407\,DBH - 0.56\,DBH^2 \quad [\text{m}] \quad \textit{Betula populifolia}
\end{aligned}
$$

In it's general form this equation uses two parameters (b_2 and b_3) that can be derived if the maximum tree height (H_{max} [m]) and diameter at breast height (DBH_{max} [cm]) values for a given species are known - assuming that these two occur at the same moment in time:

$$
\begin{aligned}
H &= 1.37 + b_2\,DBH + b_3\,DBH^2 \quad [\text{m}] \\
b_2 &= \frac{200\,(H_{max} - 1.37)}{DBH_{max}} \quad [-] \\
b_3 &= \frac{b_2}{2\,DBH_{max}} \quad [\text{cm}^{-1}]
\end{aligned}
$$

In tables A5 and A6 of appendix 2 of Bugmann (1994) an overview of the H_{max} and DBH_{max} that are to be found in the literature for *Betula pendula* are given. The mean (maximum) of these H_{max} and DBH_{max} values are 27.0 (31.0) m and 82.0 (150.0) cm, respectively. In their own model Bugmann (1994) use the average of mean and max, *i.e.*, $H_{max} = 29.0$ m and $DBH_{max} = 116.0$ cm. Figure 3 shows the resulting curves using the latter values of H_{max} and DBH_{max}:

$$
\begin{aligned}
H &= 1.37 + 0.625\,DBH - 0.00382\,DBH^2 \quad [\text{m}] \quad \textit{Betula pendula}(mean) \\
H &= 1.37 + 0.395\,DBH - 0.00132\,DBH^2 \quad [\text{m}] \quad \textit{Betula pendula}(max) \\
H &= 1.37 + 0.476\,DBH - 0.00205\,DBH^2 \quad [\text{m}] \quad \textit{Betula pendula}(mean + max)/2
\end{aligned}
$$

Also shown in are Figure 3 data from a study in eastern Germany by Knape (1996), together with an ensemble of allometric relationships for *Betula pendula* that were compiled by Scharf (2001) for Germany (dotted lines):

$$
\begin{aligned}
H &= 1.5607 + 6.5286\,\log(DBH) \quad [\text{m}] \quad (r^2 = 0.742) \quad (9.5 < DBH < 33.5cm) \\
H &= 0.6642 + 6.7311\,\log(DBH) \quad [\text{m}] \quad (r^2 = 0.816) \quad (7.5 < DBH < 37.5cm) \\
H &= 3.4022 + 6.2140\,\log(DBH) \quad [\text{m}] \quad (r^2 = 0.549) \quad (8.5 < DBH < 37.5cm) \\
H &= 3.2453 + 6.0089\,\log(DBH) \quad [\text{m}] \quad (r^2 = 0.632) \quad (7.5 < DBH < 28.5cm) \\
H &= 0.0424 + 7.1387\,\log(DBH) \quad [\text{m}] \quad (r^2 = 0.598) \quad (11.5 < DBH < 36.5cm) \\
H &= 5.1173 + 4.6099\,\log(DBH) \quad [\text{m}] \quad (r^2 = 0.5253) \quad (7.5 < DBH < 38.5cm) \\
H &= 0.3029 + 6.5326\,\log(DBH) \quad [\text{m}] \quad (r^2 = 0.6241) \quad (7.5 < DBH < 33.5cm)
\end{aligned}
$$

Oinas and Sikanen (2000) provide the following H to DBH relationship for birch:

$$
H = 1.3 + \exp\left(3.47 - \frac{16.36}{DBH + 5} - \frac{10.76}{(DBH + 5)^2}\right) \quad [\text{m}]
$$

Alternatively, Pacala et al. (1993) and Pacala et al. (1996) describes the growth of *Betula alleghaniensis* as:

$$
H = 23.2\left(1. - \exp^{\frac{-1.87\,DBH}{23.2}}\right) \quad [\text{m}]
$$

where the 23.2 refers to the maximum attainable height for that species. By using the same estimator of H_{max} (29 m) for *Betula pendula* that was used by Bugmann (1994), a height curve can be derived that is in reasonable agreement with actual height data for *Betula papyrifera*, *Betula pendula* and *Betula alleghaniensis* collected at various locations by Comeau et al. (1999), Viherä-Aarnio and Velling (1999), Heräjärvi (2001), Halliwell, D. H. and Apps, M. J. (1997), and Wang and Kimmins (2002). Furthermore this height curve does not decrease at larger DBH values:

$$H = 29.0\left(1. - \exp^{\frac{-1.87\,DBH}{29.0}}\right)\ [\mathrm{m}] \quad \textit{Betula pendula}$$

Most of the above relationships are displayed in the graph of Figure 3. Caution should be used when applying these relationships since they are based on only a few H versus DBH measurements of *Betula pendula* trees (Viherä-Aarnio and Velling 1999).

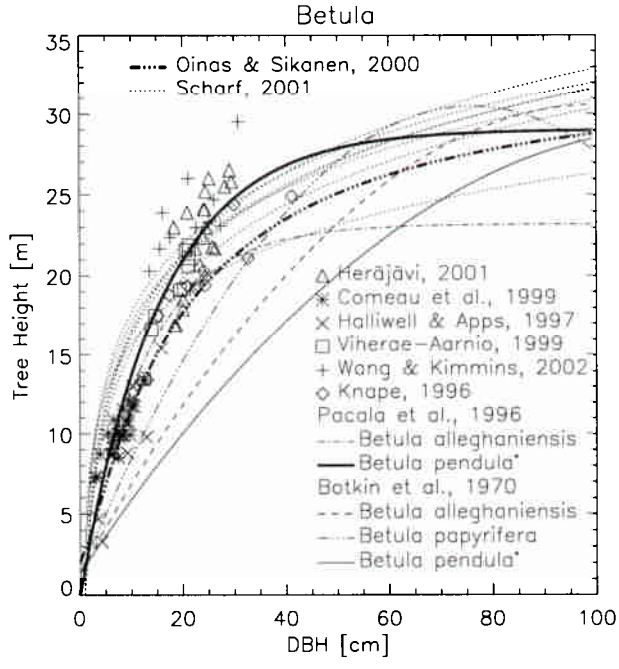

Figure 3: Tree height curve for various birch species according to the JABOWA (Botkin, 1993) and SORTIE (Pacala et al., 1993) model formulations. A '*' indicates that the relationship for *Betula pendula* was derived by using an H_{max} value of 29.0 m, and an DBH_{max} value of 116 cm for that species – both of which were taken from the appendix of Burgmann, 1994.

2.3 Height to crown, H_t [m]

The allometric formulation of Nagel et al. (2002) for the prediction of the height to the tree crown (H_t) can be used if the maximum height of the trees in the plot at the age of 100 years (H_{100}) is known:

$$H_t = H\left(1. - \exp^{-|1.3298 + 0.2577\,\frac{H}{DBH} - 0.003778\,DBH + 0.6697\,\log(H_{100})|}\right)\ [\mathrm{m}]$$

Figure 4 shows this relationship by setting H_{100} equal to the maximum tree height for *Betula pendula* ($H_{max} = 29.0$ m) as provided by Bugmann (1994). When comparing the bottom height of the crown with that of the tree itself, one notices that for small tree heights the crown length is unrealistically small. A somewhat larger crown is feasible with the relationship of Pacala et al. (1993) for *Betula alleghaniensis*:

$$H_t = 0.54\,H \quad [\mathrm{m}]$$

Figure 4 shows this relationship when applied to the tree height estimates of the same author as defined in equation 1. Again, it should be kept in mind, that the height to the bottom of the tree crown depends on the density of trees in a stand, as well as, the resulting availability of light and the tolerance to shade of the species under consideration.

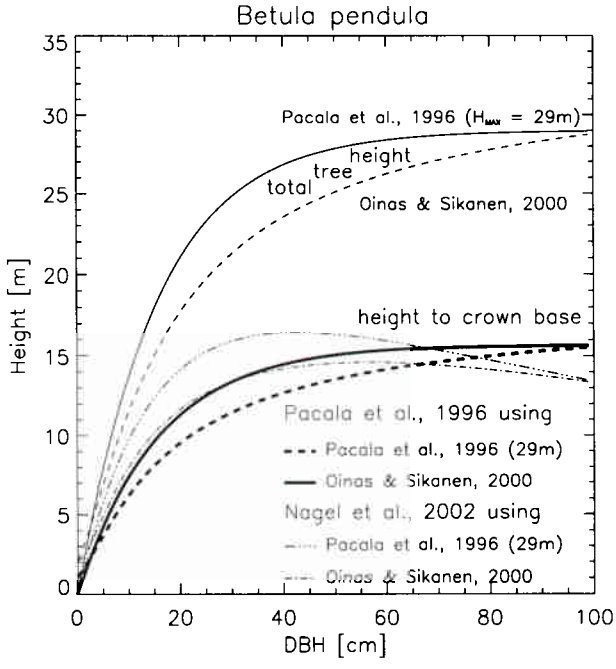

Figure 4: Allometric relationships for the height to the bottom of the crown for *betula pendula* according ot the relationships of Nagel et al., (2002) and Pacala et al., (1993). For reference, the total tree heights according to Pacala et al., (1996) and Oinas and Sikanen (2000) are also shown.

2.4 Height to the maximum crown width, H_{Cr} [m]

According to the crown model shown in the left hand graph of Figure 3 the maximum height of the crown occurs at: $H_{Cr} = H_t + 0.5\,H_{cb}$ where H_{cb} covers 36% of the total crown length H_c. However, other slightly different crown shapes may be feasible, thus shifting the height to the maximum crown radius.

2.5 Height to first dead branch, H_{nb} [m]

No information regarding the height to the first dead branch was found in the literature.

2.6 Maximum crown radius, C_r [m]

Webster and Lorimer (2003) provide the following crown radius to DBH relationship for *betula alleghaniensis*:

$$C_r = \sqrt{\frac{0.204334\, DBH^{1.489}}{\pi}} \quad [\text{m}] \tag{1}$$

Alternatively Pacala et al. (1993) describes the crown radius for *betula alleghaniensis* as:

$$C_r = 0.109\, H \quad [\text{m}] \tag{2}$$

The allometric formulation of Nagel et al. (2002) for the prediction of the crown radius is:

$$C_r = 0.1617 + 0.1030\, DBH$$

This is not too different from the crown radius estimate of Bragg (2001) for yellow birch (*Betula alleghaniensis*), who provide another crown-width estimation for paper birch (*Betula papyrifera*):

$$C_r = \frac{1}{2}\left(0.723785 + 0.666365\, DBH^{0.677279}\right) \quad [\text{m}] \quad \textit{Betula alleghaniensis} \tag{3}$$

$$C_r = \frac{1}{2}\left(1.933184 + 0.04892\, DBH^{1.325343}\right) \quad [\text{m}] \quad \textit{Betula payrifera}$$

All of these relationships are shown in Figure 5 together with actual data from Halliwell, D. H. and Apps, M. J. (1997)

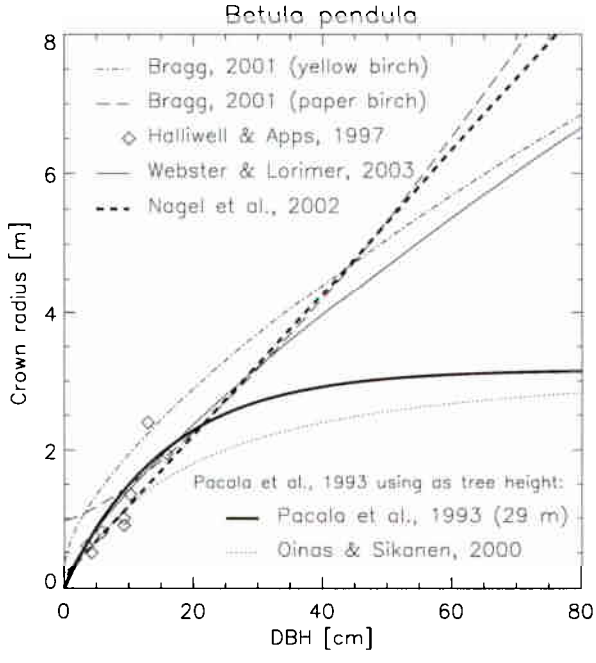

Figure 5: Allometric relationships for the radius of the tree crown of *betula alleghaniensis* according to Pacala et al., (1993), Nagel et al., (2002), Webster and Lorimer (2003), as well as some data from Halliwell and Apps, 1997.

2.7 Leaf Area Index, LAI [tree^{-1}]

The (one sided) leaf area (A_l) of young Birch stands can be described according to the information in appendix 4 of Bugmann (1994):

$$A_l = 0.028\, DBH^{1.43} \quad [\mathrm{m^2\,tree^{-1}}] \tag{4}$$

Martin et al. (1998) describes a leaf area - DBH relationship for *Betula lenta* as (dashed line in the left hand panel of Figure 6):

$$A_l = 0.148252\, DBH^{2.008} \quad [\mathrm{m^2\,tree^{-1}}] \tag{5}$$

The average leaf area index of a typical beech tree of height H can thus be obtained by dividing the above estimates of A_l by the downward projected surface area of that tree ($\pi\, C_r^2$). The right hand panel of Figure 6 shows a series of LAI estimates derived from equations 4 and 5 for the leaf area, as well as equations 1, 2 and 3 for the crown radius. It can be seen that the leaf area relationship of Bugmann (1994) yields an increase of the LAI value at small DBH values (this was true for all equations of C_r even though only one such example is presented in figure 6). Data points for paper birch at two different sites in Central British Columbia (Comeau et al. 1999), as well as for a *betula pubescens* stand in Central Siberia—mean height 15m; tree density 4600 stem/ha and mean DBH 15cm—(Röser et al. 2002) are also provided.

An empirical relationship was fitted (thick line) such as 1) to reflect the observed data as well as some of the trends in the above allometric relationships, and 2) to yield the maximum attainable LAI for beech trees (5.59) according to Tiangxiang et al. (2002) at the maximum value for the diameter at breast height (DBH_{max} = 116 cm) of Bugmann (1994):

$$LAI = 0.65\, DBH^{0.43} \quad [\mathrm{tree^{-1}}]$$

It should be noted that during the course of a year the LAI of any given birch tree changes as a function of time, and modulations of the above LAI function should thus be performed to account for this.

2.8 Foliage and Biomass

The leaves of *Betula pendula* are oval to triangular in shape, measure between 2.5 - 5 cm in length and about 3 cm in width. For *Betula pubescens* the leaf length is 1.5 to 5.5 cm and its width around 3 cm. Joosten and Lehtonen (2002) presented data of total dry biomass for birch trees in Finland that can be approximated with the following relationship:

$$W_t = 0.3\, DBH^{2.22} \quad [\mathrm{kg\ tree^{-1}}]$$

Martin et al. (1998) produced an allometric relationship for *Betula lenta* in the Appalachian region of the United States. His tree samples covered DBH values up to about 40 cm (see dashed line in Figure 7. He noted large differences in the specific leaf area for this birch species, ranging from 161.8 to 538.2 [cm^2 g^{-1}].

$$W_t = 0.0564937\, DBH^{2.726} \quad [\mathrm{kg\ tree^{-1}}]$$

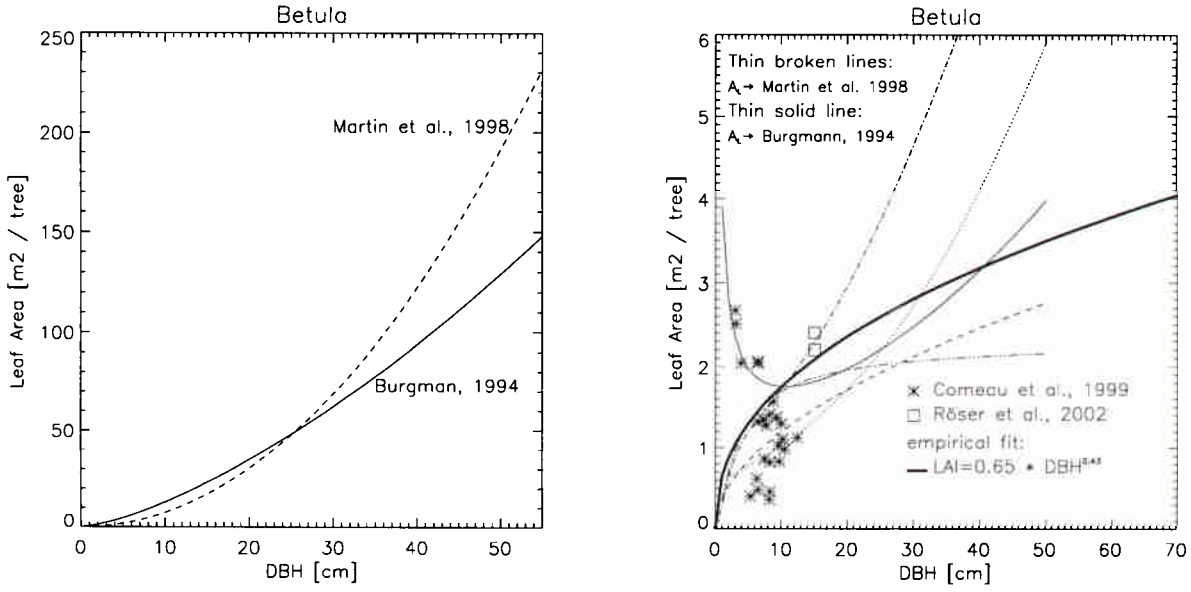

Figure 6: Left panel: One sided leaf area (A_l) for birch, as derived from the relationships of Bugmann (1994) and Martin et al. (1998). Right panel: One sided leaf area index per tree, derived from the ratio of A_l and A_r (the downward projected crown area). Estimates of the latter quantity used the crown radius C_r relationships of Webster and Lorimer (2003), Pacala et al., (1996) and Nagel et al (2002) to compute the downward-projected crown area: $A_r = \pi C_r^2$. Data from Comeau et al. (1999) and Röser et al. (2002) are provided. The empirical fit was obtained by forcing the maximum LAI value (5.59) for beech (Tianxiang et al., 2002) to occur at the maximum DBH value (116 cm) of Bugmann (1994).

Jenkins et al. (2003) give the following equation for the dry biomass of *betula* in the USA:

$$W_t = 0.133627\, DBH^{2.4342} \quad [\text{kg tree}^{-1}] \qquad (r^2 = 0.981)$$

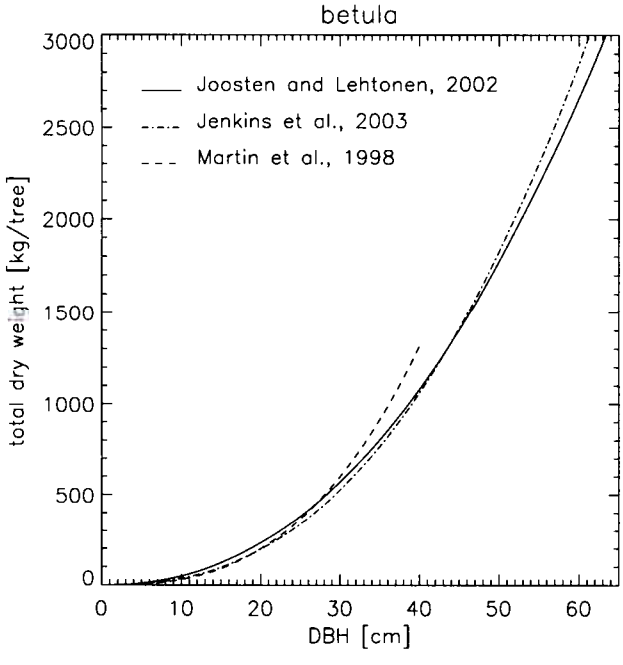

Figure 7: Allometric relationships for total dry weight of birch trees in Finland (Joosten and Lehtonen, 2002), as well as, birch in general (Jenkins et al., 2003) and *Betula lenta* (Martin et al., 1998) in the United States.

3 European Beech (*Fagus Silvatica*)

The naturally distribution of the European beech ranges from the southern tip of Scandinavia, through middle and western Europe, and some of the higher elevation locations of southern Europe. In the northern Alps and the Appennines, for example, the European beech can exists at altitude up to about 1600 - 1800 m, respectively (Röhrig 1980).

3.1 Crown shape

European beech trees are relatively tolerant to shade as well as winter frost. They grow best if sufficient water is available and continue to do so for a very long time. Often the European beech occurs together with other tree species in the same stand, whether this is with Norway spruce in mountainous areas, or with the larch, ash, maple, elm, lime and cherry trees (Röhrig 1980). Due to the closed crown layer in many beech forests little light is available for the understory and consequently these forest types are often devoid of large bushes. The crown shape of the beech can be represented using a hemispherical and a conical element, as outlined by Pretzsch (1992). The base of the hemisphere touches the base of the conical section at a height H_{Cr}, forming the widest part of the crown as indicated in the middle panel of Figure 8. The right hand panel in the same Figure shows a 3-D visualization of a mature beech stand with a somewhat more differentiated crown shape representation.

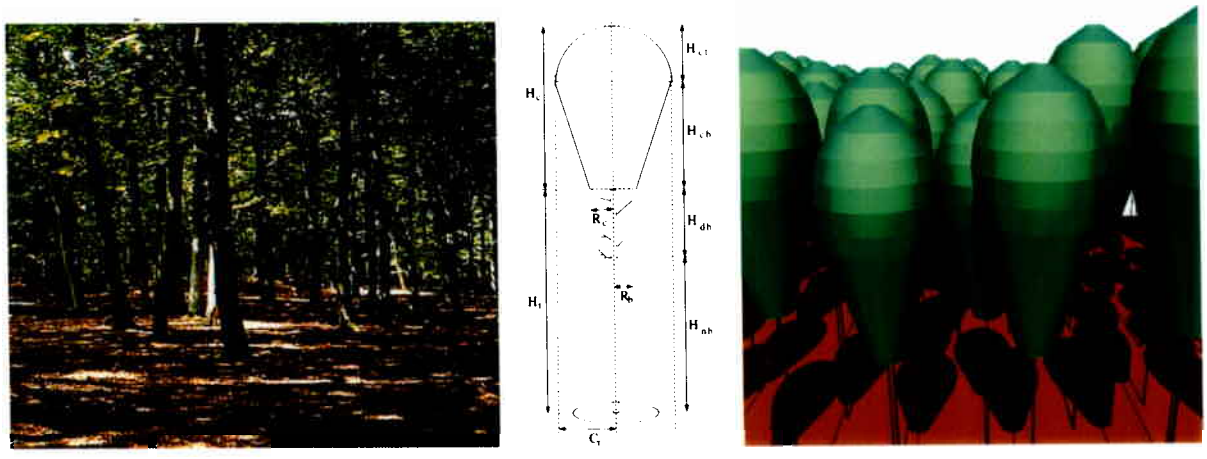

Figure 8: Left panel: European beech forest photographed by Anna-Lena Anderberg, (Source: `http://linnaeus.nrm.se/flora/`). Middle panel: Crown model of *Fagus sylvatica* after Pretzsch, 1992. Right Panel: 3-D visualization of a 20 m high beech stand for which the reflectance fields can be modelled using the radiation transfer model of Govaerts and Vertstraete, 1998.

Pretzsch (1992) provides two equations to describe the crown radius 1) r_t from the top of the crown down to the maximum crown radius C_r, and 2) r_b from the largest lateral extent of the crown down to the bottom of the crown (d [m] is the distance from the crown top downwards):

$$r_t = \frac{C_r}{\sqrt[3]{H_{ct}}} d^{\frac{1}{3}} \quad [\text{m}]$$

$$r_b = C_r - \frac{R_c - C_r}{H_c - H_{ct}} H_{ct} + d \frac{R_c - C_r}{H_c - H_{ct}} \quad [\text{m}]$$

3.2 Tree height, H [m]

The total tree height H for *Fagus silvatica* in north-western Germany has been related by Guericke (2001) to the trunk diameter at breast height (DBH [cm]) on the basis of tree height

measurements between 10 and ~40 m (or DBH values between 8 and ~70 cm) with $r^2 = 0.8664$ in his figure 4-22:

$$H = 11.447 \ln(DBH) - 11.885 \quad [\text{m}]$$

However, since this equation does not offer suitable tree height estimates below about 7 m, a linear approximation is proposed to bridge the gap (compare with thick grey line in the right hand panel of Figure 9):

$$H = 1.37 + 1.28855\,DBH \quad [\text{m}] \qquad\qquad 0 < DBH < 7.0\,[\text{cm}]$$

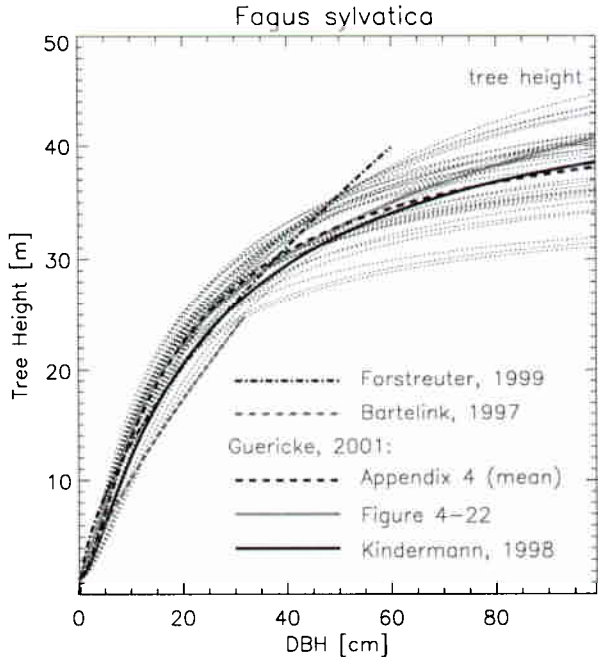

Figure 9: Tree height - DBH relationship of Guericke, 2001: thin dotted lines are all the data of his appendix 4, the thick black dashed line was generated with the mean parameters of his appendix 4, and the thick grey line is his logarithmic equation of Figure 4-22 (with a linear cut-off below DBH=7 cm). Also provided is the relationship of Kindermann, 1998, Bartelink, 1997 and Forstreuter, 1999.

In his appendix 4 Guericke (2001) provides further biometric estimates of the tree height distribution with DBH using the equation of Kramer (1982) (thin black lines in the right hand panel of Figure 9), *i.e.*:

$$H = 1.3 + \left(\frac{DBH}{a_0 + a_1\,DBH}\right)^2 \quad [\text{m}]$$

By averaging the various coefficients of a_0 and a_1 in the appendix 4 of Guericke (2001) a tree height curve can be obtained (thick dashed line in right hand panel of Figure 9) that is in agreement with the author's logarithmic equation from figure 4-22 (see above) with the additional benefit that the lower tree heights are provided as well:

$$H = 1.3 + \left(\frac{DBH}{1.31811 + 0.151515\,DBH}\right)^2 \quad [\text{m}]$$

For comparison the allometric relationship of Kindermann (1998) for a 93 year old stand are also provided in Figure 9:

$$H = 1.3 + \frac{DBH^2}{2.07 + 0.507\,DBH + 0.0215\,DBH^2} \quad [\text{m}]$$

Similarly the relationship derived by Bartelink (1997) for a stand with $2 < DBH < 32$ cm ($r^2 = 0.934$) in the Netherlands is provided:

$$H = 1.732 + DBH^{0.769} \quad [\text{m}]$$

Forstreuter, M (1999) provides several allometric equations for biomass estimations that allow to construct a tree height-DBH relationship (shown as a dash-dotted line in Figure 9):

$$H = 3.240838\,DBH^{0.613065} \quad [\text{m}]$$

3.3 Height to crown, H_t [m]

The allometric equation describing the relationship between $DBH > 8.71$ cm and the height to the tree crown (H_t) of figure 4-22 from Guericke (2001) ($r^2 = 0.462$) is:

$$H_t = 5.6627\,\ln(DBH) - 5.9119 \quad [\text{m}]$$

In his appendix 4 Guericke (2001) provides further biometric estimates of the height-to-the-crown distribution with DBH using the equation of Van Deusen and Bigin (1985) (thin dotted lines in the right hand panel of Figure 10):

$$H_t = H * \left(1 - \exp^{-\left(b_0 + b_1 \frac{H}{DBH}\right)^2}\right) \quad [\text{m}]$$

By selecting a 'best' couple of the b_0 and b_1 coefficients from appendix 4 of Guericke (2001) a crown height curve can be obtained (thick grey line in Figure 10) that follows closely the logarithmic curve of the same authors and accounts for the observed spread of his data at higher DBH values:

$$H_t = H\left(1 - \exp^{-\left(0.950735 - 0.0812830 \frac{H}{DBH}\right)^2}\right) \text{[m]} \qquad DBH \geq 0.11055 \text{ [cm]}$$

$$H_t = 0.0 \text{ [m]} \qquad DBH < 0.11055 \text{ [cm]}$$

This relation is also very close to that provided by Pretzsch et al. (2002) ($r^2 = 0.73$) and indicated as a thick black line with long dashes in the right hand panel of Figure 10:

$$H_t = H\left(1 - \exp^{-(0.5478 + 0.1094 \frac{H}{DBH} + 0.0023\,DBH)}\right) \quad [\text{m}]$$

Bartelink (1997) provides a relationship for a beech stand in the Netherlands ($2 < \text{DBH} < 30$ cm) that allows for the computing of H_t (see long dashed lines in Figure 10):

$$H_t = H - (2.897 + 0.0112469\,DBH^2) \quad [\text{m}]$$

Again, it should be kept in mind, that the height to the bottom of the tree crown depends on the density of trees in a stand, as well as, the resulting availability of light and the tolerance to shade of the species under consideration.

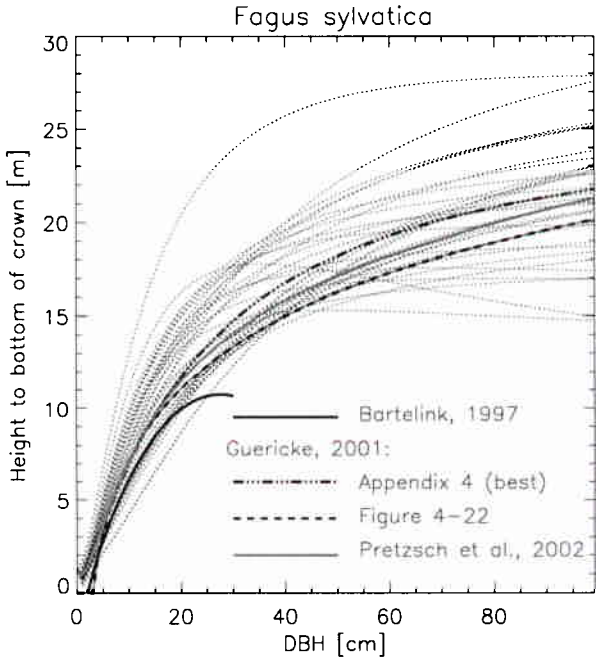

Figure 10: Ensemble of allometric relationships from appendix 4 (dotted lines) of Guericke (2001) for the 'height to the bottom of the tree crown' H_t, together with the 'best' estimate thereof and another logarithmic equation from Figure 4-22 of the same author. The relationship of Bartelink (1997) and that of Pretzsch et al. (2002) are also shown.

3.4 Height to the maximum crown width, H_{Cr} [m]

In figure 4-40 and table 4-15 Guericke (2001) describes the relationship between H and the height to the maximum crown diameter ($H_{Cr} = H_t + H_{cb}$) as follows ($r^2 = 0.90$):

$$H_{Cr} = 0.7874\,H \; + \; 0.5441 \quad [\mathrm{m}]$$

However, Pretzsch (1992) simplifies this by saying that $H_{Cr} = H_t + 3H_c/5$ where $H_c = H - H_t$). Figure 11 shows that this approximation (dashed line) is acceptable. Thus:

$$H_{Cr} \;=\; H_t + 3\,\frac{H - H_t}{5} \quad [\mathrm{m}]$$

3.5 Height to first dead branch, H_{nb} [m]

The allometric equation describing the relationship between $DBH > 6.72$ cm and the height to the first dead branch (H_{nb}) was taken from figure 4-22 of Guericke (2001) ($r^2 = 0.4963$):

$$\begin{aligned} H_{nb} &= 6.1522\ln(DBH) - 11.718\,[\mathrm{m}] && 6.72 \le DBH\,[\mathrm{cm}] \\ H_{nb} &= 0.0\,[\mathrm{m}] && DBH < 6.72\,[\mathrm{cm}] \end{aligned}$$

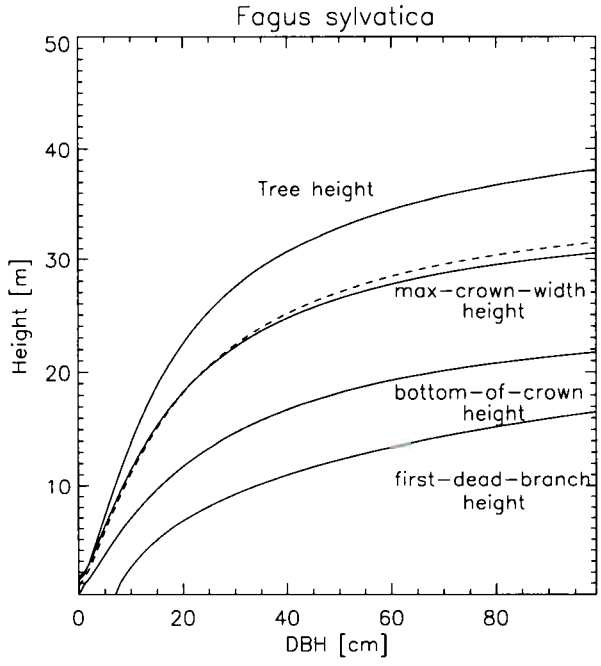

Figure 11: Allometric relationships (solid lines) of Guericke, (2001) for 'tree height' H, 'bottom of crown height' H_t, 'height to the maximum crown width' H_{Cr}, and 'height to first dead branch' H_{nb}, as well as, the simplified approach (dashed line) of Pretzsch (1992) for H_{Cr}.

3.6 Maximum crown radius, C_r [m]

In figure 4-27 and table 4-9 Guericke (2001) describes the relationship between tree height H and maximum crown diameter $(2 * C_r)$ [m] ($r^2 = 0.77$) as (compare with Figure 12):

$$C_r = 0.0821\, DBH + 0.7694\,[\text{m}]$$

This equation holds well when compared to the mean ($C_r = 0.078307\, DBH + 0.905689\,[m]$) of a series of estimates of C_r for individual stands from appendix 4 of Guericke (2001). Note however that C_r does not go to zero as $DBH \rightarrow 0$ (see Figure 12). This is not the case for the allometric relation of Nagel et al. (2002) which increases slowly at small heights to become equivalent to the functions of Guericke (2001) at larger DBH values (solid black line in Figure 12):

$$C_r = (1.04185 + 0.075\, DBH)\left(1 - \exp^{-\left(\frac{DBH}{5.7292}\right)^{1.3341}}\right) \text{ [m]}$$

Bartelink (1997) provides a relationship for a beech stand in the Netherlands (2 < DBH < 30 cm) that allows for the computing of C_r (see short dashed lines in Figure 12):

$$C_r = \sqrt{\frac{1}{\pi}\left(\frac{8.560 + 0.0286\, DBH^{2.623}}{3.38}\right)^{0.98232}} \text{ [m]}$$

3.7 Bottom crown radius, R_c [m]

According to Pretzsch (1992) the radius of the tree crown at the bottom of the crown (that is at height H_t) can be approximated with (see Figure 12):

$$R_c = C_r/3 \quad [\mathrm{m}]$$

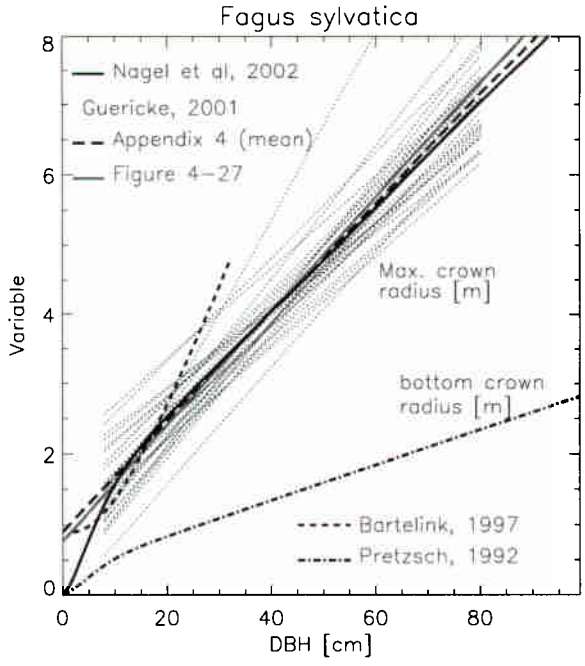

Figure 12: Allometric relationships of Guericke (2001), Bartelink (1997), and Nagel et al. (2002) for the maximum crown radius, C_r, as well as, the relationship of Pretzsch (1992)—applied to C_r of Nagel et al. (2002)—for the radius of the crown at its lower end, R_c.

3.8 Leaf Area Index, LAI [tree^{-1}]

The (one sided) leaf area (A_l) of young Beech stands was estimated by Prskawetz and Lexer (2000) for 12 pure stands in central Europe using:

$$A_l = 0.307279\, DBH^{1.803} \quad [\mathrm{m}^2\ \mathrm{tree}^{-1}]$$

The average leaf area index of a typical beech tree of height H can thus be obtained by dividing the above by the downward projected surface area of that tree ($\pi\, C_r^2$) - where we used ($C_r = 0.078307\, DBH + 0.905689\,[m]$) the mean relationship from the appendix of Guericke (2001) in Figure 13:

$$LAI = \frac{0.307279\, DBH^{1.803}}{\pi\,(0.078307\, DBH + 0.905689)^2} \quad [\mathrm{tree}^{-1}]$$

The relationship of Burger 1949 for leaf area per tree (A_l) [m^2] shows good agreement over its verified range ($DBH < 50$ cm) when compared to the leaf area index per tree estimate of Prskawetz and Lexer (2000), ($LAI = A_l/(\pi\, {C_r}^2)$):

$$LAI = \frac{1.187\,DBH + 0.0955\,DBH^2 + 0.00095\,DBH^3}{\pi\,C_r{}^2} \quad [\text{tree}^{-1}]$$

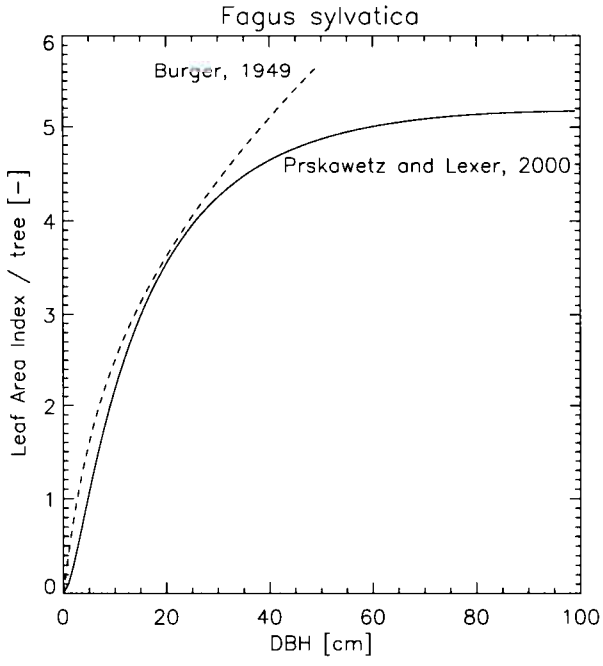

Figure 13: Leaf area index (LAI) derived from the allometric relationship for one sided leaf area A_l of 1) Burger (1949), and 2) Prskawetz and Lexer (2000), using the mean relationship from the data in the appendix of Guericke, (2001) for the maximum crown radius C_r to compute the (circular) downward-projected crown area: $A_r = \pi\,C_r^2$

To account for the dynamical behaviour of the LAI during the growing season of a mixed oak/beech forest, Muusche et al. (2001) proposed in their case study to describe the temporal behaviour of the LAI as:

$$LAI = -7.87 + 0.12\,t_d - 0.00027\,t_d^2 \quad [\text{tree}^{-1}]$$

where t_d is the day-number in the year ($0 \rightarrow 365$). However, such a seasonal variation in LAI is highly dependent on both climatic and geographic effects as well as the various factors affecting the local site conditions.

3.9 Foliage and Biomass

The leaves of *Fagus sylvatica* are elliptical in shape, 5 to 10 cm long and approximately 5 cm wide. Bartelink (1997) provides a series of relationships to estimate the dry weight of the foliage W_f, branches W_b, crown W_c, trunk W_s and the total tree W_t [$kg\,tree^{-1}$]. His dataset applies to a beech stand in the Netherlands with $2 <$ DBH < 30 cm. Relying only on DBH resulted in:

$$\begin{aligned}
W_f &= 0.375 + 0.0024\,DBH^{2.517} && r^2 = 0.906 && [\text{kg tree}^{-1}] \\
W_b &= 0.0020\,DBH^{3.265} && r^2 = 0.916 && [\text{kg tree}^{-1}] \\
W_c &= 0.0031\,DBH^{3.161} && r^2 = 0.924 && [\text{kg tree}^{-1}] \\
W_s &= 0.0762\,DBH^{2.523} && r^2 = 0.979 && [\text{kg tree}^{-1}] \\
W_t &= 0.0798\,DBH^{2.601} && r^2 = 0.988 && [\text{kg tree}^{-1}]
\end{aligned}$$

whereas using DBH and tree height (H) values yielded:

$$
\begin{aligned}
W_f &= 0.0167\, DBH^{2.951}\, H^{-1.101} \quad r^2 = 0.923 \quad [\mathrm{kg\,tree^{-1}}] \\
W_b &= 0.0114\, DBH^{3.682}\, H^{-1.031} \quad r^2 = 0.920 \quad [\mathrm{kg\,tree^{-1}}] \\
W_c &= 0.0183\, DBH^{3.614}\, H^{-1.078} \quad r^2 = 0.929 \quad [\mathrm{kg\,tree^{-1}}] \\
W_s &= 0.0109\, DBH^{1.951}\, H^{1.262} \quad r^2 = 0.996 \quad [\mathrm{kg\,tree^{-1}}] \\
W_t &= 0.0306\, DBH^{2.347}\, H^{0.590} \quad r^2 = 0.991 \quad [\mathrm{kg\,tree^{-1}}]
\end{aligned}
$$

Figure 14 shows the results of the above equations over their valid range of DBH values—between 2 and 32 cm—together with two equations provided by Forstreuter, M (1999) to estimate the total dry weight W_t [kg/tree] aboveground:

$$
\begin{aligned}
W_t &= 0.1293\, DBH^{2.44} \quad [\mathrm{kg\,tree^{-1}}] \quad r^2 = 0.98 \\
W_t &= 0.0012\, H^{3.98} \quad [\mathrm{kg\,tree^{-1}}] \quad r^2 = 0.96
\end{aligned}
$$

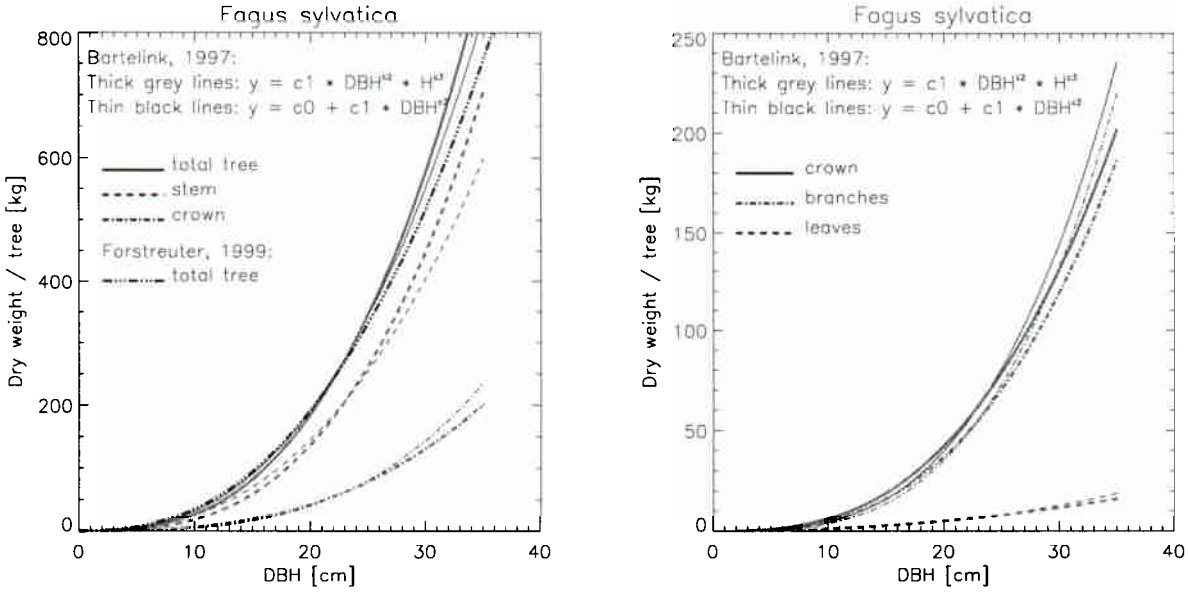

Figure 14: Allometric relationships of Bartelink (1997) for estimating the dry weight of the foliage, branches and the total crown (left hand panel), as well as for the tree trunk and the total above ground dry weight of the tree (right hand panel). The equations were derived from a beech stand in the Netherlands having $2 < \mathrm{DBH} < 32$ cm. Also shown is the relationship of Forstreuter (1999) for total aboveground dry weight (left hand panel).

4 European Larch (*Larix decidua*)

Like all other existing larch species, the natural distribution of the European larch is restricted to the northern hemisphere, and this primarily to the boreal range of coniferous forests in Russia, and the alpine and sub-alpine region of mountainous areas like the Alps and Tatra. Whereas in the eastern Alps and lower Tatra, larch trees occur at elevations from 400 to 1000 m, they are equally well encountered at greater heights and occasionally even up to altitudes of 2400 m (Röhrig 1980).

4.1 Crown shape

European larch trees are relatively demanding as regards the availability of light. They are pioneer trees that occupy empty tracts of land such as those cleared by avalanches, and can proliferate well in dry mountainous areas. Within mixed stands the European larch can only succeed if (due to its initial rapid growth) it remains free from too much shadowing (Röhrig 1980). Naturally grown larch stock in mountainous areas are thus relatively sparse in density and often have a dense undergrowth. Due to the lower early growth-rate (and the substantial shade-tolerance) of the beech, the European larch is often mixed with this species. The crown shape of the European larch can be represented using two conical elements, as outlined by Pretzsch (1992). The bases of these conical elements are touching and form the widest part of the crown as indicated in the middle graph of Figure 15. The right hand panel in the same Figure shows a 3-D visualization of a mature Larch stand with a somewhat more differentiated crown shape representation.

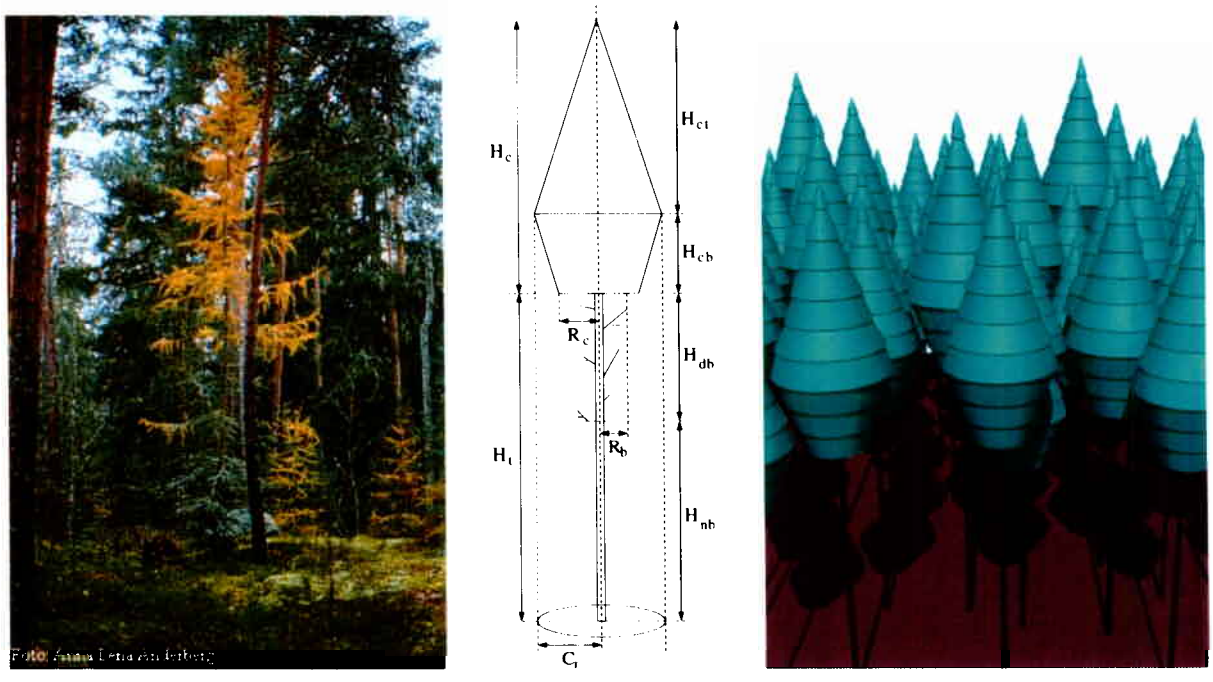

Figure 15: Left panel: Autumnal larch tree with yellowish needles photographed by Anna-Lena Anderberg, (Source: `http://linnaeus.nrm.se/flora/`). Middle panel: Crown model of *Larix decidua* after Pretzsch, 1992. Right Panel: 3-D visualization of a 20 m high larch stand for which the reflectance fields can be modelled using the radiation transfer model of Govaerts and Vertstraete, 1998.

4.2 Tree height, H [m]

Lischke et al. (1998) propose a Ker-Smith equation to relate the total tree height H for *Larix decidua* to the trunk diameter at breast height (DBH [cm]) for a stand with a maximum tree height of 52 m and a maximum DBH of 185 cm:

$$H = 1.37 + 2(52.0 - 1.37)\frac{DBH}{185} - (52.0 - 1.37)\left(\frac{DBH}{185}\right)^2 \text{ [m]}$$

Guericke (2001) relates total tree height H to the DBH [cm] on the basis of tree height measurements between 16 and ~40 m (or DBH values between 20 and ~70 cm) in his figure 4-22 ($r^2 = 0.6497$):

$$H = 17.795 \ln(DBH) - 37.317 \text{ [m]}$$

It can be seen in Figure 16 that the Ker-Smith equation of Lischke et al. (1998) (dotted line) continuously underestimates the tree heights for $DBH > 20$ cm when compared to the relationship of Guericke (2001). Shao, G. (1986) also noted this behaviour (especially for small and medium sized trees). However, given the near-linear rise of the Ker-Smith equation below DBH values of 20 cm, one could relate the tree height linearly between the $H = 1.37$ m value (at $DBH = 0$ cm) and the $H = 16.8$ m value (at $DBH = 21$ cm) from the equation of Guericke (2001):

$$\begin{aligned} H &= 17.795 \ln(DBH) - 37.317 \text{ [m]} && 20.0 \leq DBH \text{ [cm]} \\ H &= 0.73876\, DBH + 1.37 \text{ [m]} && DBH \leq 20.0 \text{ [cm]} \end{aligned}$$

An alternative allometric relationship is that provided by Kindermann (1998) for a 93 year old stand (see long dashed line in Figure 16) ($\sigma_{fit} = \pm 3.12m$):

$$H = 1.3 + \frac{1}{\left(0.155 + \frac{1.47}{DBH}\right)^2} \text{ [m]}$$

4.3 Height to crown, H_t [m]

The allometric equation describing the relationship between $DBH > 8.71$ cm and the height to the tree crown (H_t) was taken from figure 4-22 of Guericke (2001) ($r^2 = 0.4532$):

$$\begin{aligned} H_t &= 13.337 \ln(DBH) - 28.860 \text{ [m]} && 8.71 \leq DBH \text{ [cm]} \\ H_t &= 0.0 \text{ [m]} && DBH < 8.71 \text{ [cm]} \end{aligned}$$

4.4 Height to the maximum crown width, H_{Cr} [m]

In his figure 4-40 and table 4-15 Guericke (2001) describes the relationship between H and the height to the maximum crown diameter ($H_{Cr} = H_t + H_{cb}$) as follows ($r^2 = 0.93$):

$$H_{Cr} = 0.8925\, H - 2.8278 \text{ [m]}$$

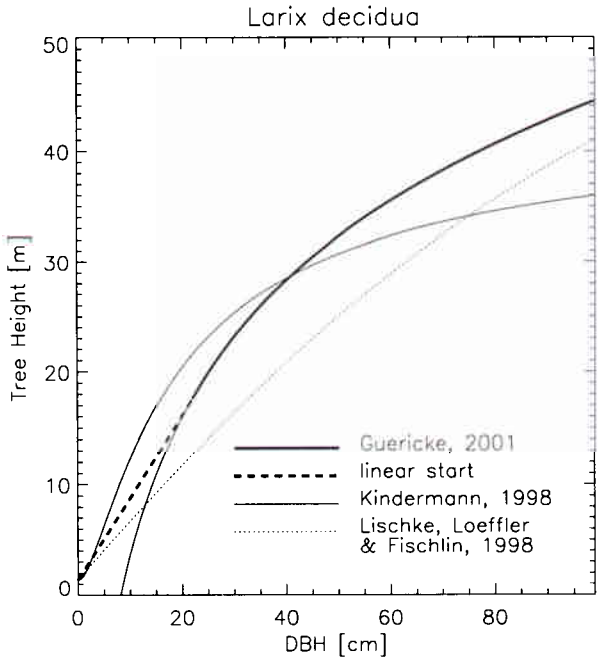

Figure 16: The DBH-tree height relationship for European larch according to Guericke (2001) , Lischke et al. (1998), and Kindermann (1998). Also shown is the linear approximation below DBH=20 cm for the Guericke curve (small dashed line).

However, the same author then utilizes the simplified approach of Pretzsch (1992) who maintains that $H_{Cr} = H_t + H_c/3$ (for *picea abies*) where $H_c = H - H_t$). Figure 17 shows that this approximation (dashed line) is indeed acceptable for *larix decidua*. Thus:

$$H_{Cr} = H_t + \frac{H - H_t}{3} \text{ [m]}$$

4.5 Height to first dead branch, H_{nb} [m]

The allometric equation describing the relationship between $DBH > 22.18$ cm and the height to the first dead branch (H_{nb}) was taken from figure 4-22 of Guericke (2001) ($r^2 = 0.2528$):

$$\begin{aligned} H_{nb} &= 10.224 \ln(DBH) - 31.688 \text{ [m]} && 22.18 \leq DBH \text{ [cm]} \\ H_{nb} &= 0.0 \text{ [m]} && DBH < 22.18 \text{ [cm]} \end{aligned}$$

4.6 Maximum crown radius, C_r [m]

In his figure 4-27 and table 4-9 Guericke (2001) describes the relationship between tree height H and maximum crown diameter ($C_D = 2C_r$) [m] ($r^2 = 0.71$) as (see grey dashed line in Figure 18):

$$C_r = 0.0707\, DBH - 0.0729 \text{ [m]}$$

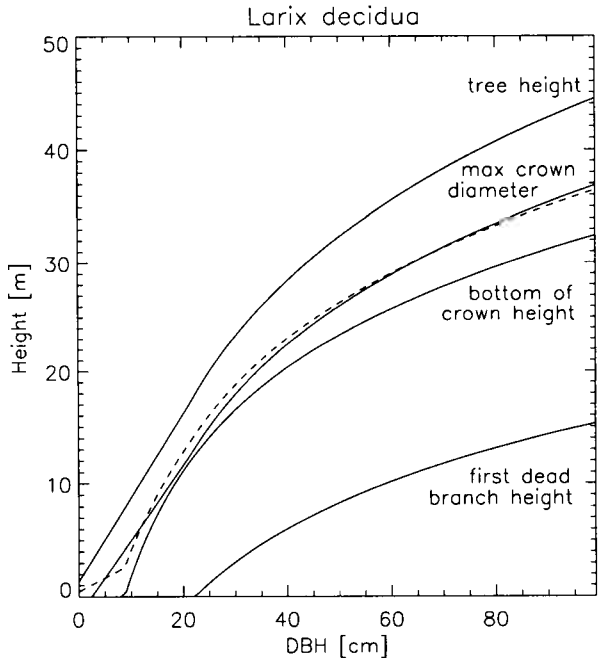

Figure 17: Allometric relationships for European larch of Guericke (2001) for 'height to bottom of crown' H_t, 'height to the maximum crown diameter' H_{Cr}, and 'height to first dead branch' H_{nb}, as well as, the simplified approach (dashed line) of Pretzsch (1992) for H_{Cr}.

This simple equation holds well when compared to a series of estimates of C_r for individual stands from appendix 4 of Guericke (2001), even though it is less than zero for values of DBH smaller than 1.03 cm (compare with dotted lines in Figure 18). Note that from amongst the ensemble of dotted lines the ones with the smallest slopes have been derived from populations with the greatest range of DBH values (10 - 75 cm). For example, plot 310, which does not deliver negative values of C_r as $DBH \rightarrow 0$, yields (r^2=0.66):

$$C_r = 0.0540\, DBH + 0.07947\,[\mathrm{m}]$$

Interestingly, Nagel et al. (2002) provides a non-linear relationship that mimics this behaviour:

$$C_r = (1.84810 + 0.0381\, DBH)\left(1 - \exp^{-\left(\frac{DBH}{21.8046}\right)^{1.53}}\right) \;\; [\mathrm{m}]$$

4.7 Bottom crown radius, R_c [m]

According to Pretzsch (1992) the radius of the tree crown at the bottom of the crown (that is at height H_t) can be approximated with (see Figure 18):

$$R_c \;=\; C_r/2.\,[\mathrm{m}]$$

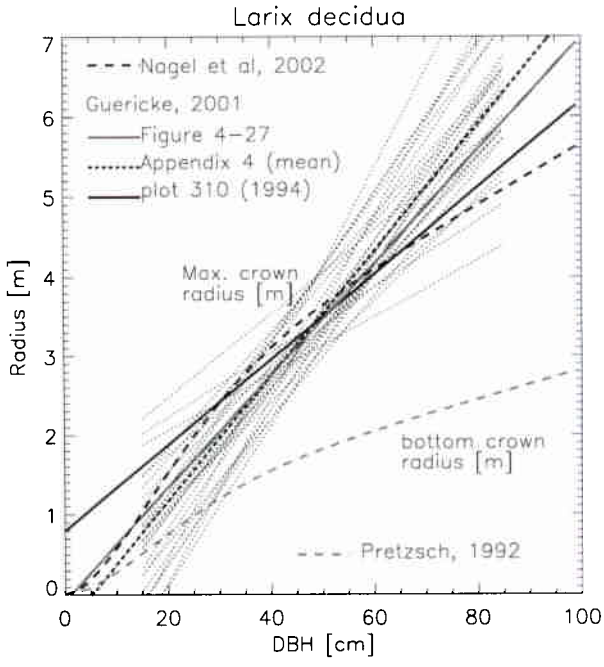

Figure 18: DBH-maximum crown radius relationships for European larch according to Guericke (2001). Shown are the data from his appendix 4 and his figure 4-27. The relationship of Nagel et al. (2002) for the maximum crown radius is also provided. In addition Pretzsch (1992) was used to compute the value of the lower crown radius R_c from the latter estimate of C_r.

4.8 Leaf Area Index, LAI [tree^{-1}]

Very limited information as to the leaf area index of European larch trees was found in the literature. Burger (1945) provided an equation to determine the one sided leaf area of larch trees (A_l [m^2 tree^{-1}]):

$$A_l = \frac{1}{2}\left(1.174\,DBH + 0.046\,DBH^2 + 0.0007\,DBH^3\right) \quad [\mathrm{m^2\,tree^{-1}}]$$

The left hand panel of figure 19 shows that relationship together with some data points from the study of Gower et al. (1999), and an allometric expression of the latter Gower et al. (1993) for the one sided leaf area of *Larix decidua* (solid line):

$$A_l = 0.006\,DBH^{2.921} \quad [\mathrm{m^2\,tree^{-1}}] \qquad (r^2 = 0.902)$$

The deviations between the two curves could for example result due to geographic and temporal differences in the foliage characteristics of larch trees.

To convert the leaf area per tree into an estimate of the leaf area index per tree, one has to divide A_l by the downward projected surface area of that tree ($\pi\,C_r^2$). In the case of larch most of the equations that were provided previously to compute the crown radius did not allow for a well behaved LAI - DBH relationship (see, for example, the dashed lines in the right hand panel of Figure 19. In the case of the data provided by Guericke (2001) (C_r–DBH relationships in his Figure 4-27 and the mean of his Appendix 4) this misbehaviour related to the fact that these linear relationships were generally derived for values of DBH lying between 20 and 80 cm, and often yielded very small or even negative crown radii values as $DBH \rightarrow 0$.. The same issue arose with the crown radius equation of Nagel et al. (2002). However, in order to provide at least an indication of a possible LAI-DBH relationship for the European larch, the solid lines in

Figure 19 were derived from the linear relationship for C_r of plot 310 in Appendix 4 of Guericke (2001). The thick version of this line relates to the leaf area estimate of Burger (1945), whereas the thin solidline relates to A_l of Gower et al. (1993). The latter relationship—although stringly increasing at larger DBH values—has the benefit that it agrees reasonably well with the stated LAI of 5.1 ± 0.1 that was provided by Gower et al. (1993) for their stand with a mean DBH around 24cm.

$$LAI = \frac{A_l}{\pi\,(0.054\,DBH + 0.7947)^2} \quad [\text{tree}^{-1}]$$

It should be noted that during the course of a year the LAI of any given larch tree changes as a function of time. Appropriate modulations of the above LAI function for a given tree height have to be performed.

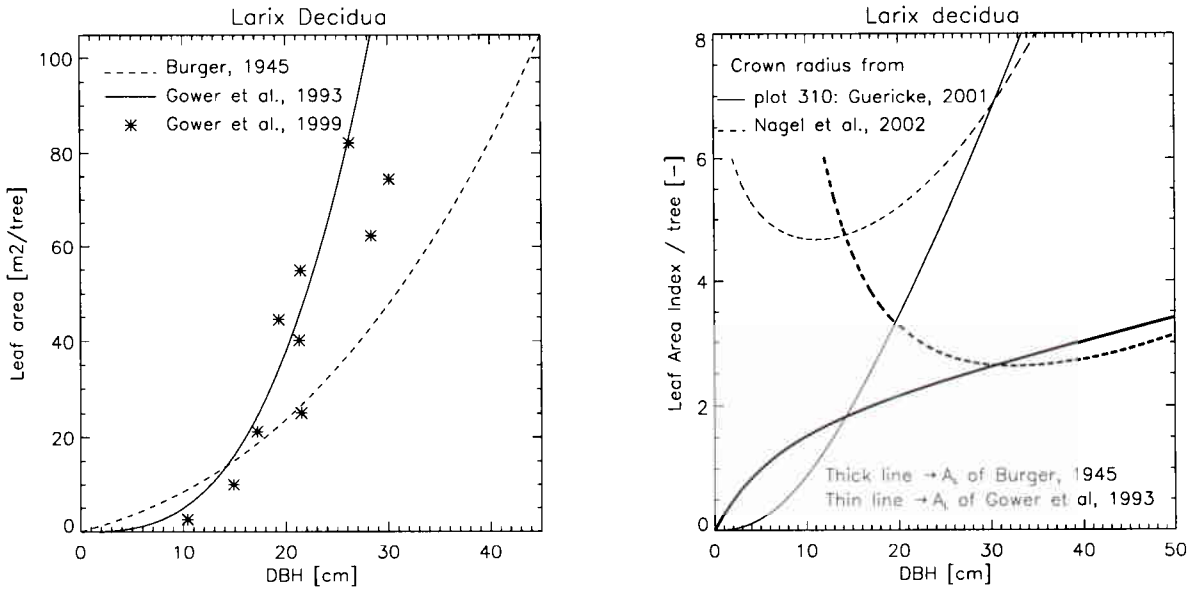

Figure 19: Left panel: Allometric relationships of Burger (1945) and Gower et al (1993) describing the one sided leaf area (A_l) for European larch. Also shown are data from Gower et al. (1999). Right panel: The one sided leaf area index per tree as derived from 1) the allometric equations of Burger (1945) and Gower et al., (1993) for leaf area, and 2) the maximum crown radius equations of Guericke, (2001) and Nagel et al. (2002) to compute the (circular) downward-projected crown area. It can be seen that under these conditions the crown radius equation of Nagel et al, (2002) does not deliver reasonable LAI estimates at medium to small DBH values.

4.9 Foliage and Biomass

The needles of *Larix decidua* are typically 15-30 mm long and about 0.5-0.8 mm wide. Kajimoto et al. (1999) provides the following estimates for stem W_s , branch W_b and needle W_f dry weight for *Larix gmelinii* for a stand with a mean (maximum) height of 5.5 (11.2) m, a mean (maximum) DBH of 6.8 (18.5) cm and a tree density of 1910 stems/hectare:

$$W_s = 0.1680\,DBH^{2.978} \quad [\text{kg tree}^{-1}] \qquad (r^2 = 0.98)$$

$$W_b = 0.0545\,DBH^{2.846} \quad [\text{kg tree}^{-1}] \quad (r^2 = 0.98)$$
$$W_f = 0.0222\,DBH^{2.788} \quad [\text{kg tree}^{-1}] \quad (r^2 = 0.98)$$

Figure 20 shows the sum of the above equations, *i.e.*, the total aboveground biomass $W_t = W_s + W_b + W_f$ [kg / tree] as well as the same parameter estimated with the equation of Jenkins et al. (2003) for cedar/larch species in the USA:

$$W_t = 0.130864\,DBH^{2.2592} \quad [\text{kg tree}^{-1}] \quad (r^2 = 0.981)$$

Gower et al. (1993) provides a series of allometric equations that allow to estimate the dry weight for the stem (W_s), the live (W_{lb}) and dead (W_{db}) branches, as well as the foliage (W_f) of *Larix decidua* trees:

$$W_s = 0.248313\,DBH^{2.111} \quad [\text{kg tree}^{-1}] \quad (r^2 = 0.974)$$
$$W_{lb} = 0.000553\,DBH^{3.423} \quad [\text{kg tree}^{-1}] \quad (r^2 = 0.964)$$
$$W_{db} = 0.001770\,DBH^{2.850} \quad [\text{kg tree}^{-1}] \quad (r^2 = 0.523)$$
$$W_f = 0.000492\,DBH^{2.912} \quad [\text{kg tree}^{-1}] \quad (r^2 = 0.907)$$

The total above ground dry weight for *Larix decidua*, $W_t = W_s + W_{lb} + W_{db} + W_f$ can thus be computed (see Figure 20).

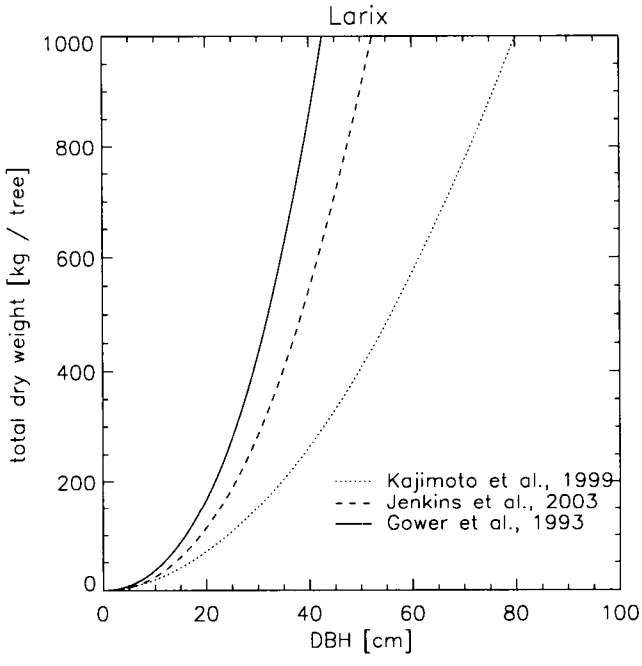

Figure 20: Total aboveground dry weight for 1) *Larix decidua* according to Gower et al. (2003), 2) cedar/larch trees in the USA according to Jenkins et al., (2003) and 3) *Larix gmelinii* in Siberia according to Kajimoto et al., (1999).

5 Norway Spruce (*Picea Abies*)

Norway spruce is naturally distributed across Scandinavia, the Baltic States and further east beyond the Ural mountains. It is also encountered in parts of middle and south-eastern Europe as well as in smaller pockets across former Yugoslavia and the Carpathian Mountain range (Röhrig 1980). Norway spruce can be encountered close to sea-level in the North and up to an elevation of 2200 m in the Alps (Schmidt-Vogt 1976).

5.1 Crown shape

Norway spruce trees are relatively tolerant to shade. Young trees are often amongst the understory or middle layer of mixed stands (containing, for example, fir, pine and beech). Although it tends to occur naturally in coldish continental climates, Norway spruce has proven very apt to central European climate conditions (Röhrig 1980). The crown shape of the Norway spruce is predominantly conical, with broad crowns occurring in lower altitudes of central Europe and tall and pointy crowns at higher elevations or further to the north. Pretzsch (1992) represents the crown shape of the Norway Spruce using two conical elements although representations of a cone on top of a cylinder were used by Chen et al. (1997) for black spruce. The bases of these conical elements are touching and form the widest part of the crown as indicated in the middle panel of Figure 21.
The right hand panel in the same Figure shows a 3-D visualization of a mature Norway spruce stand with a somewhat more differentiated crown shape representation.

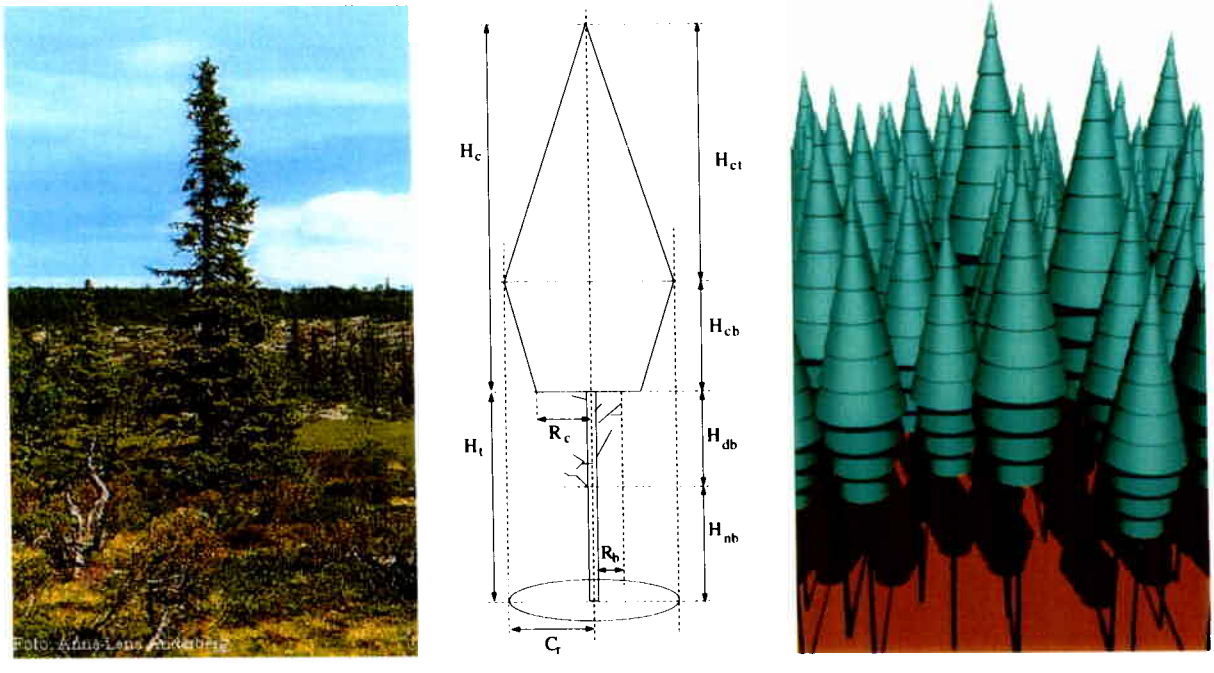

Figure 21: Left panel: Mature Norway spruce photographed by Anna-Lena Anderberg, (Source: `http://linnaeus.nrm.se/flora/`). Middle panel: Crown model of *Picea abies* after Pretzsch, 1992. Right Panel: 3-D visualization of a 20 m high Norway spruce stand for which the reflectance fields can be modelled using the radiation transfer model of Govaerts and Vertstraete, 1998.

Pretzsch (1992) provides two equations to describe the crown radius: 1) r_t from the top of the crown down to the maximum crown radius C_r, and 2) r_b from the largest lateral extent of the crown to the bottom of the crown (d is the downward distance from the top of the crown):

$$r_t = \frac{C_r}{H_{ct}} d \quad [\text{m}]$$

$$r_b = C_r - \frac{R_c - C_r}{H_c - H_{ct}} H_{ct} + d \frac{R_c - C_r}{H_c - H_{ct}} \quad [\text{m}]$$

5.2 Tree height, H [m]

The total tree height H for *Picea abies* in Finland has been related by Siipilehto (2000) to the trunk diameter at breast height (DBH [cm]) using Näslund's height curve:

$$H = 1.3 + \left(\frac{DBH}{1.811 + 0.308\,DBH}\right)^3 \quad [\text{m}]$$

Oinas and Sikanen (2000) provide the following H to DBH relationship for spruce:

$$H = 1.3 + \exp\left(3.71 - \frac{22.88}{DBH + 5} - \frac{24.75}{(DBH + 5)^2}\right) \quad [\text{m}]$$

Kindermann (1998) provides two allometric relationships for the tree height, one exponential – with the standard deviation of the fit being $\sigma = \pm 3.07$ m – that was retrieved from a 63 year old Norway spruce stand in Austria:

$$H = 1.3 + \exp\left(3.85 - \frac{19.5}{DBH}\right) \quad [\text{m}]$$

and another with a better standard deviation of the fit ($\sigma = \pm 1.62$ m) from a 98 year old stand (solid line in Figure 22):

$$H = 1.3 + \left(\frac{DBH^2}{6.22 + 0.131\,DBH + 0.0317\,DBH^2}\right) \quad [\text{m}]$$

5.3 Height to crown, H_t [m]

An allometric equation describing the relationship between DBH and the height to the tree crown (H_t) is given by Pretzsch et al. (2002) with $r^2 = 0.79$ (see Figure 23):

$$H_t = H\left(1 - \exp^{(-0.0443 - 0.8823\frac{H}{DBH} - 0.0004\,DBH)}\right) \quad [\text{m}]$$

5.4 Height to the maximum crown width, H_{Cr} [m]

Pretzsch (1992) indicates that the height to the maximum crown width for Norway spruce is $H_{Cr} = H_t + H_c/3$ where $H_c = H - H_t$ (compare with Figure 23):

$$H_{Cr} = H_t + \frac{H - H_t}{3} \quad [\text{m}]$$

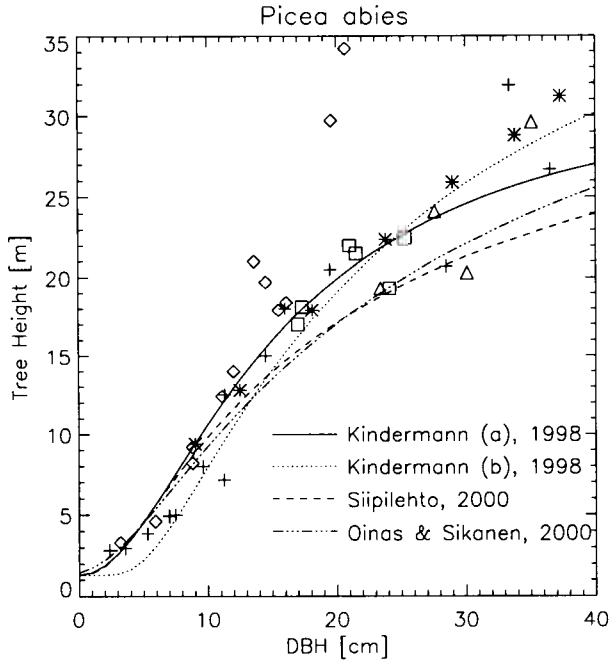

Figure 22: Allometric DBH-tree height relationship for Norway spruce according to Siipilehto (2000) together with 2 allometric relationships from Kindermann (1998), and that of Oinas and Sikanen (2000). Also shown are data from a variety of sources in the literature.

5.5 Height to first dead branch, H_{nb} [m]

Schmidt (2001) provides two empirical relationships (equations 31 and 32) that can be utilized to compute the height to the lowest dead branch:

$$\begin{aligned} H_{nb} &= H_{gb}\left(\exp^{\frac{(0.523\,H)^{1.7}}{1000}} - 1\right) \quad [\mathrm{m}] \\ H_{gb} &= H_t\,(1 - 0.359\,\exp^{-0.0807\,H_t}) \quad [\mathrm{m}] \end{aligned}$$

where H_{gb} is an estimate of the lowest green branch - which can be situated below what Schmidt (2001) terms the height to the bottom of the crown. Nevertheless H_{nb} if computed by equation 6 differs only minimally whether using H_{gb} or the actual H_t.

5.6 Maximum crown radius, C_r [m]

Nagel et al. (2002) describes the relationship between tree height H and the maximum crown diameter ($C_D = 2\,C_r$) [m] as (thin line in Figure 24):

$$C_r = (0.6122 + 0.0536\,DBH) \quad [\mathrm{m}]$$

Equation 12 in Pretzsch et al. (2002) uses an exponential relationship to come to a very similar result (compare with thick line in Figure 24). Using the parameter in table 8 of their appendix ($r^2 = 0.73$):

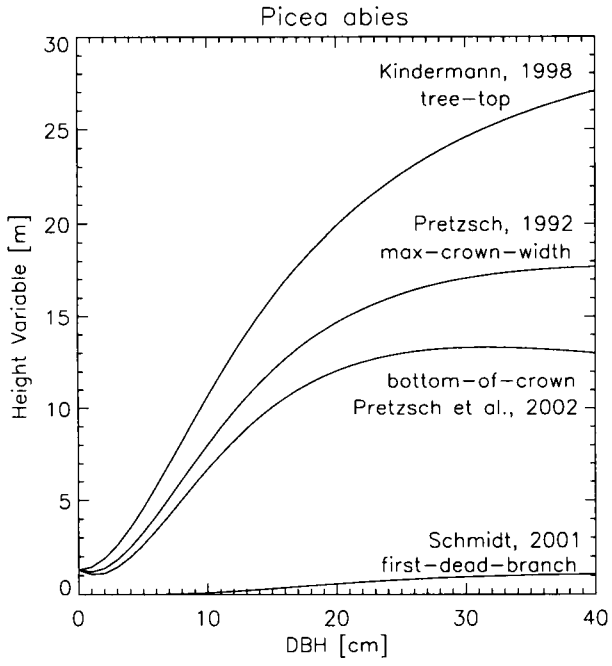

Figure 23: Allometric relationships for Norway spruce describing 1) the 'height-to-tree-top' H (Kindermann, 1998), 2) the 'height-to-bottom-of-crown' H_t (Pretzsch et al., 2002), 3) the 'height-to-maximum-crown-width' H_{Cr} (Pretzsch, 1992), and 4) the 'height to the first dead branch' H_{nb} (Schmidt, 2001).

$$C_r = \frac{1}{2} \exp\left(0.2195 + 0.2545 \ln(DBH) + 0.009\,H - 0.6735 \ln \frac{H}{DBH}\right) \quad [\mathrm{m}] \quad (6)$$

5.7 Bottom crown radius, R_c [m]

According to table 2.1 of Pretzsch (1992) the crown radius at the bottom of the tree crown (that is at height H_t) can be approximated with (see Figure 24):

$$R_c = C_r/2. \quad [\mathrm{m}]$$

5.8 Leaf Area Index, LAI [tree^{-1}]

Many authors have provided estimates for biomass or leaf area rather than the leaf area index (per tree) itself. Burger (1941a), for example, provided two relationships between the (one sided) leaf area A_l [m^2/tree] and the DBH [cm] that have been verified empirically up to $DBH \approx 50cm$:

$$A_l = 1.4375\,DBH + 0.074\,DBH^2 \quad [\mathrm{m^2\,tree^{-1}}] \quad (a)$$
$$A_l = -0.6245\,DBH + 0.287\,DBH^2 - 0.00023\,DBH^3 \quad [\mathrm{m^2\,tree^{-1}}] \quad (b)$$

Grote (1999) uses an exponential relationship to relate foliage biomass W_l [kg/tree] with the DBH [cm]. The (single sided) foliage area A_l [m^2/tree] can then be retrieved if the one-sided specific leaf area value ($SLA_p = PLA/W_l$ [m^2/kg]) is known: $A_l = W_l\,SLA_p$ - with PLA [m^2]

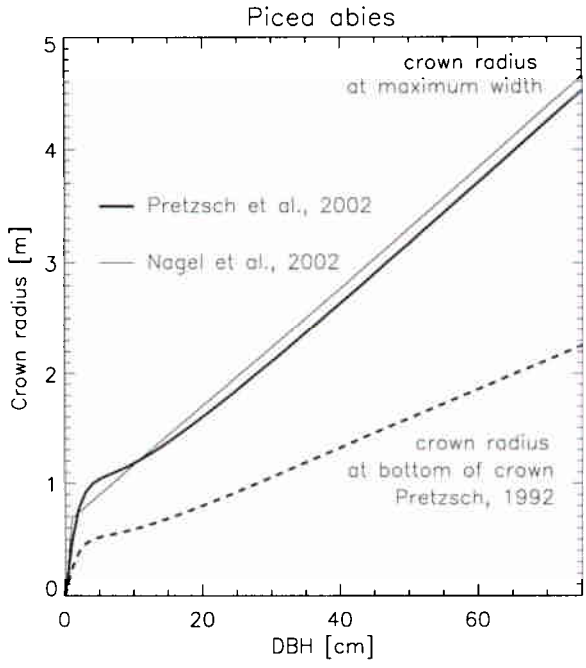

Figure 24: The allometric relationships between the DBH [cm] and the maximum crown radius C_r for Norway spruce, as implemented in the SILVA model (Pretzsch et al., 2002) and the BWINPro6.1 model (Nagel et al., 2002). Also shown is the relation of Pretzsch (1992) for the lower crown radius R_c from the estimate of C_r of Pretzsch et al. (2002).

being the projected needle area. To obtain the one sided specific needle area we assume all needles to be flat, *i.e.*, $SLA_p \approx SLA/2$. A large dispersion of specific total leaf area values SLA (accounting for the total *i.e.*, double sided, needle area) has been indicated in the literature, *e.g.*, 5.9 m^2/kg by Johansson (1999), 12.4 m^2/kg by Burger (1941a), and 3.0 m^2/kg by Gower et al. (1993). In the following SLA_p thus refers to half of the values of Johansson (1999) unless indicated otherwise.

The relationship of Grote (1999) has only been validated empirically for trees between $8 \leq DBH \leq 20$ cm (furthermore A_l does not tend to zero as $DBH \to 0$).

$$A_l = 9.363\, SLA_p\, \exp^{0.00109956\, DBH^2} \quad [\mathrm{m^2\, tree^{-1}}]$$

Nilson et al. (1999) uses an equation from Marklund (1988) together with their estimate of the SLA_p (6.58 m^2/kg) to retrieve the leaf area A_l [m^2/tree]:

$$A_l = 0.207381\, SLA_p\, \exp^{\frac{8.4127\, DBH}{DBH+12}}\, H^{-1.5628}\, H_c^{1.4032} \quad [\mathrm{m^2\, tree^{-1}}]$$

where H_c is the length of the crown. Obviously the values for A_l depend on what we use as the bottom of the crown to determine the crown length $H_c = H - H_t$ or $H_c = H - H_{gb}$. Similarly the choice of the value for the SLA_p matters. In the left hand panel of Figure 25, H_{gb} and (half of) the SLA value of the authors themselves was used.

Johansson (1999) provides another relationship that has the advantage that $A_l \to 0$ as $DBH \to 0$ and furthermore that A_l assymptotically reaches a maximum value for large values of DBH (this is unlike some of the relationships seen before), and finally it has been empirically verified for

$4.9 \leq DBH \leq 33.0$ cm (see solid line in the left hand panel of Figure 25:

$$A_l = 36.2826\, SLA_p\, (1 - \exp^{-0.08\, DBH}\,)^{2.1576} \quad [\mathrm{m^2\, tree^{-1}}]$$

The allometric expression of Gower et al. (1993) for the one sided leaf area of *Picea Abies* is:

$$A_l \;=\; 0.13366\, DBH^{2.163} \quad [\mathrm{m^2\, tree^{-1}}] \qquad (r^2 = 0.952)$$

The right hand panel of Figure 25 shows an estimate of the leaf area index as derived from the leaf area estimate of Johansson (1999) —SLA_p = 2.95 $\mathrm{m^2/kg}$ —and the projected Crown Area was computed with the C_r values of Pretzsch et al. (2002). The long dashed (dotted) line describes the proposed relationship within (outside) the available range of DBH values (6 - 33 cm). Some data points as presented by Johansson (1999) are also shown.

$$LAI \;=\; 136.28\, \frac{(1 - \exp^{-0.08\, DBH}\,)^{2.1576}}{{C_r}^2} \quad [\mathrm{tree^{-1}}]$$

Figure 25 also shows a possible $DBH - LAI$ relationship, computed with the leaf area relation of Gower et al. (1993) and the downward projected crown area computed with the C_r values of Pretzsch et al. (2002) (again the dotted line indicates an extrapolation of the prescribed relationship outside the range of available data points in the study of Gower et al. 1993). The steep (flat) short dashed line in Figure 25 was constructed using the leaf area equation *a* (*b*) of Burger (1941a) (apparently valid for DBH = 0 to 50 cm) and the crown radius of Pretzsch et al. (2002) (to estimate C_r). Finally, the two allometric $DBH - LAI$ equation of the study of Küssner and Mosandl (2000)—who measured half of the actual surface area of the concave needles of Norway spruce to compute the equivalent of the one-sided leaf area (of deciduous trees) from which they then obtained their allometric relationship for LAI—are also displayed in Figure 25 (as dotted lines outside the available range of DBH values (15-40 cm) for that study):

$$\begin{aligned} LAI &= 3.52 + 2.282\, \log(DBH) \quad [\mathrm{tree^{-1}}] \\ LAI &= 3.52 + 2.504\, \log(DBH) \quad [\mathrm{tree^{-1}}] \end{aligned} \tag{7}$$

A drawback of the latter equations is that they do no fall below LAI values of 3.52 as the $DBH \rightarrow 0$. A similar argument applies also to the flatter of the two $DBH - LAI$ relationships of Burger (1941a), whereas the steeper of his estimates has negative LAI values for $DBH < 2$ cm. These findings, together with the increasing and then decreasing LAI relationship derived from the A_l of Johansson (1999) are however partly due to the crown radius estimator of Pretzsch et al. (2002), and the imposed formula to compute A_l from this estimate.

The thick grey line in Figure 25 was fitted empirically to provide a single $DBH - LAI$ relationships that spanned 1) a large range of DBH values, and b) is relatively close to most of the above LAI estimations (within their range of applicability). Since several authors have noted LAI value sof 10 or above for Norway spruce (10.8 $\mathrm{m^2/m^2}$ by von Droste zu Hülshoff (1969) for a 76 year old spruce stand, 11.5 $\mathrm{m^2/m^2}$ by Nihlgård (1972) for a 55 year-old plantation of Norway spruce in southern Sweden, 9.1 - 10.6 $\mathrm{m^2/m^2}$ by Dohrenbusch et al. (1993) for a 58 year-old spruce stand.) the proposed curve was fitted alongside the estimates of Küssner and Mosandl (2000):

$$LAI = 12.25\,(1 - \exp^{-0.1\,DBH})^{1.6} \quad [\text{tree}^{-1}]$$

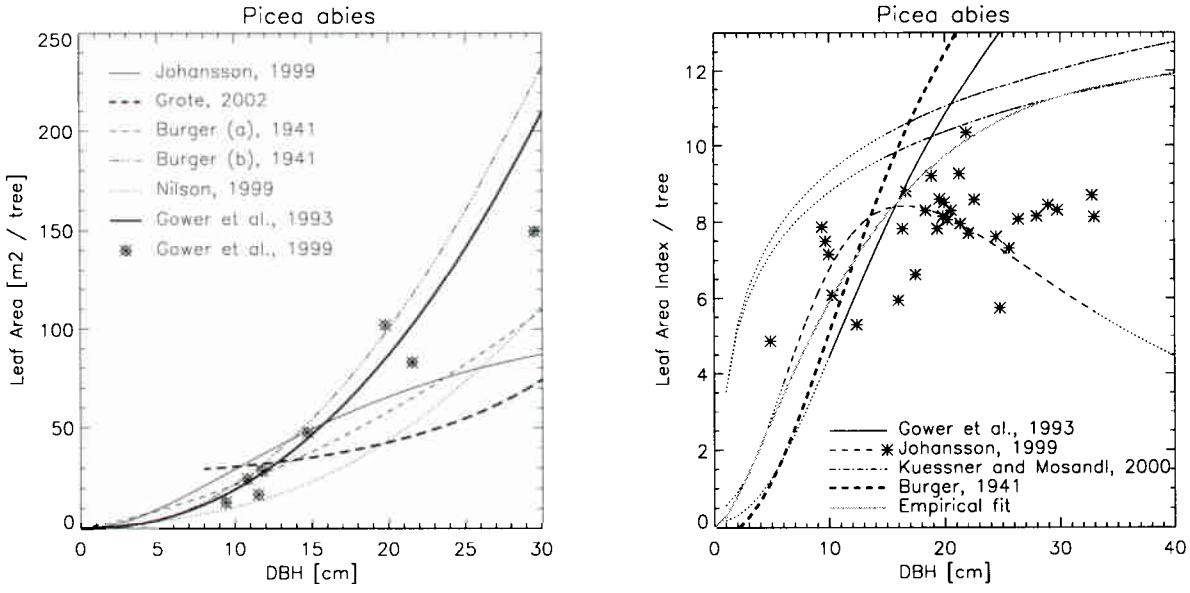

Figure 25: Left panel: The allometric relationships for Norway spruce of Johansson (1999), Nilson et al. (1999), Burger (1941), Grote (2002) and Gower et al., (1993) for the one sided leaf area (A_l) - together with data from Gower et al. (1999). Right panel: The one sided leaf area index per tree as derived from the allometric equations for A_l of Johansson (1999), Burger (1941) and Gower et al. (1993) using the crown radius (C_r) estimates of Pretzsch (2002) to compute the downward-projected crown area: $A_r = \pi\, C_r^2$. Also shown are data from Johansson (1999), the two $DBH - LAI$ relationship of Kuessner and Mosandl (2000), and an empirical fit to the available information (thick grey line). Dotted lines are extrapolations outside the range of available DBH data for the various studies.

5.9 Foliage and Biomass

Johansson (1999) reports an average needle length of 17.5 (11.6 - 21.0) mm. This corresponds to a total surface area of 52 mm^2 (or 58 mm^2 according to the formula of Kerner et al. (1977) who state that the total needle area ranges between 40 - 60 mm^2 depending on the origin of the needle in the crown). Similarly, Johansson (1999) presents a relationship between DBH [mm] and the total biomass above stump level, AGB [tons dry weight/hectare] as follows:

$$AGB = 353968\ (1 - \exp^{-0.014\,DBH})^{5.707} \quad [\text{kg ha}^{-1}]$$

The same author also provides a relationship ($r^2 = 0.975$) between DBH and the dry weight for the needles (W_f), the dry weight for the stems and twigs (W_B), as well as the total (stem + branches + needles) dry weight W_t [kg/tree], that compares well with four independently conducted studies:

$$\begin{aligned}
W_t &= 21988.7574\,(1 - \exp^{-0.0006\,DBH})^{2.44} && [\text{kg tree}^{-1}] && r^2 = 0.955 \\
W_b &= 1910.3700\,(1 - \exp^{-0.0029\,DBH})^{3.9846} && [\text{kg tree}^{-1}] && r^2 = 0.961 \\
W_f &= 36.2826\,(1 - \exp^{-0.0080\,DBH})^{2.1576} && [\text{kg tree}^{-1}] && r^2 = 0.975
\end{aligned}$$

Gower et al. (1993) provides a series of allometric equations that allow to estimate the dry weight for the stem (W_s), the live (W_{lb}) and dead (W_{db}) branches, as well as the foliage (W_f) of *Picea abies* trees:

$$
\begin{aligned}
W_s &= 0.105196\, DBH^{2.310} \quad [\mathrm{kg\,tree^{-1}}] \quad (r^2 = 0.975) \\
W_{lb} &= 0.011350\, DBH^{2.570} \quad [\mathrm{kg\,tree^{-1}}] \quad (r^2 = 0.976) \\
W_{db} &= 0.027669\, DBH^{2.226} \quad [\mathrm{kg\,tree^{-1}}] \quad (r^2 = 0.765) \\
W_f &= 0.029174\, DBH^{2.292} \quad [\mathrm{kg\,tree^{-1}}] \quad (r^2 = 0.960)
\end{aligned}
$$

The total above ground dry weight for *Picea abies*, $W_t = W_s + W_{lb} + W_{db} + W_f$ can thus be computed (see Figure 26).

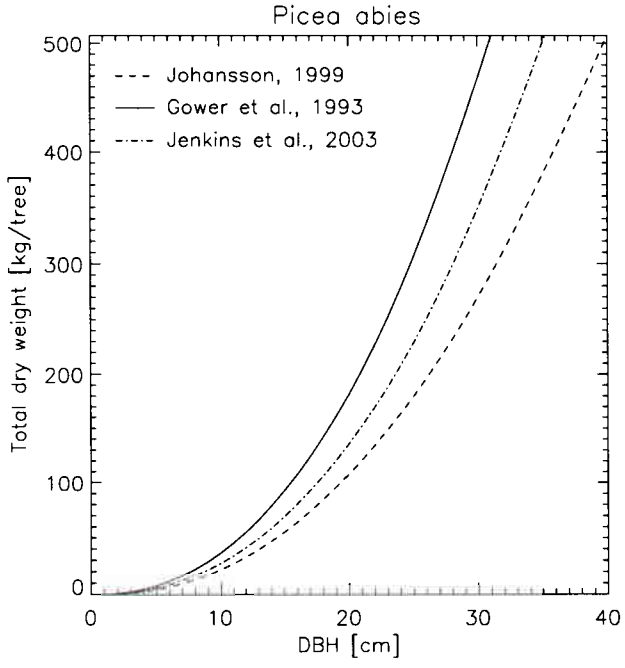

Figure 26: The total above ground dry weight for Norway spruce as described by Johansson (1999) and Gower et al. (1993), as well as the estimate of Jenkins et al (2003) for spruce species in the USA.

6 Scots Pine (*Pinus sylvestris*)

Scots pine is naturally distributed from Scotland to eastern Siberia, as well as from the boreal to the temperate vegetation zones as far south as the Sierra Nevada in Spain, or the Pontus Mountain range in Turkey (Stenberg et al. 1994, Röhrig 1980). In northern Scandinavia Scots pine forms the alpine and arctic timber line against tundra, in southern Europe it naturally occupies sites in the mountains up to an elevation of 2000 m.

6.1 Crown shape

Scots pine trees require substantial amounts of light. They are relatively resilient against cold/frost and grow both on dry and wet soils. Their growth pattern is monopodial, with young trees being approximately conical in shape. As the trees mature the crown form often becomes more rounded because elongation of the main stem is reduced relative to the laterals (Stenberg et al. 1994). The lower portion of the trunk is characterised by fissures and a dark brown (grey-brown) bark colour for young (old) trees. In the upper portion of the trunk the bark is reddish-brown in colour. The crown shape of the Scots Pine can thus be represented using two conical elements, as outlined by Pretzsch (1992), where the bases of the two conical elements are touching and form the widest part of the crown as indicated in the middle panel of Figure 27. The right hand panel in the same Figure shows a 3-D visualization of a mature Scots pine stand with a somewhat more differentiated crown shape representation.

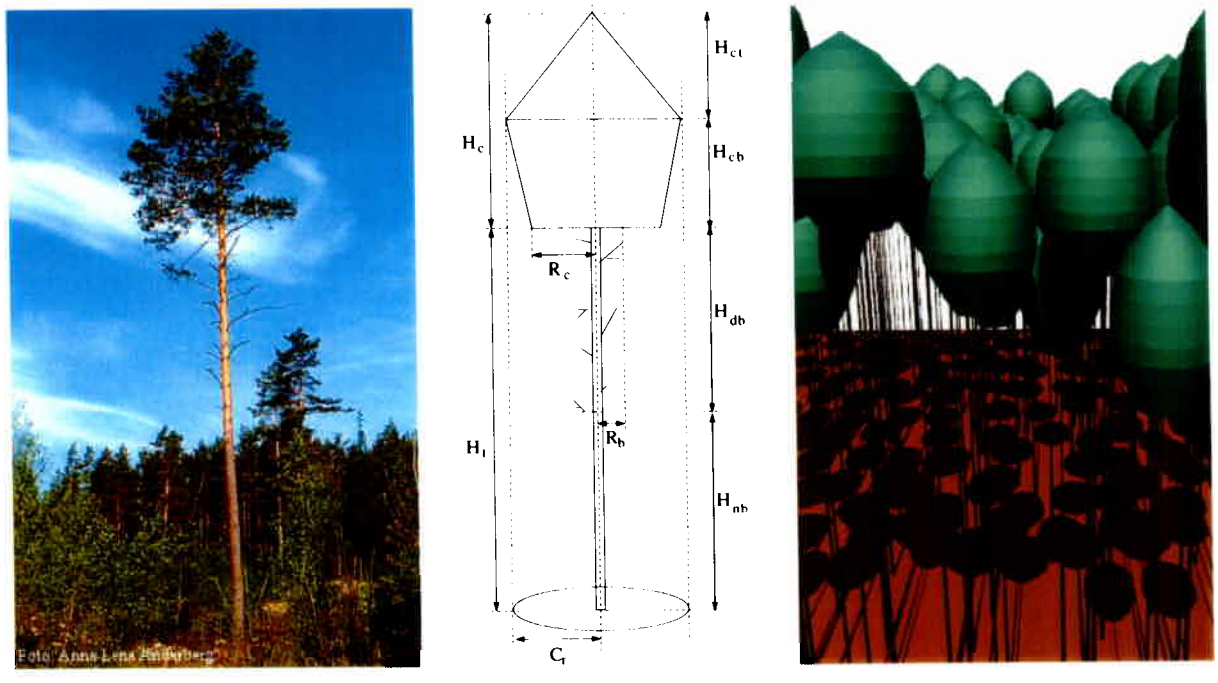

Figure 27: Left panel: Mature Scots pine photographed by Anna-Lena Anderberg, (Source: `http://linnaeus.nrm.se/flora/`). Middle panel: Crown model of *Pinus sylvestris* after Pretzsch, 1992. Right Panel: 3-D visualization of a 20 m high Scots pine stand for which the reflectance fields can be modelled using the radiation transfer model of Govaerts and Vertstraete, 1998.

6.2 Tree height, H [m]

In order to relate the total height H [m] of a *Pinus sylvestris* tree to its diameter at breast height (DBH [cm]) Kindermann (1998) applied the following allometric equation in two different stands in Germany:

$$H = 1.3 + \frac{1}{a_0 + \frac{a_1}{DBH}} \quad [\text{m}]$$

where $a_0 = 0.208$ (0.202) and $a_1 = 0.466$ (0.130) for stand A (B) and the standard deviation of the resulting fit was $\sigma = \pm 0.99$ (± 1.55) $[m]$. Sloboda (1991) provides another equation for Scots pine stands in Germany:

$$H = 1.3 + b_0 \exp^{(-b_1/DBH)} \quad [\text{m}]$$

with $b_0 = 50.532\,(49.937)$ and $b_1 = 24.88\,(30.99)$ for his first (second) stand. Figure 28 shows that these estimates differ from those of Kindermann (1998), especially at relatively small and large DBH values. Somewhat between the above estimates lies the relationship of Cermák et al. (1998), which was derived for a *Pinus sylvestris* stand in Belgium ($r^2 = 0.98$):

$$H = 24.8\,(1 - \exp^{(-DBH/14.4)})^{0.758} \quad [\text{m}]$$

Eberswalde (2001) provides the following H to DBH relationship for a mixed stand of *Pinus sylvestris* and *Pinus ponderosa* where the available DBH values of the former tree type range from 25 to 55 cm:

$$H = 1.3 + 36.21845 \exp^{\frac{-16.43036}{DBH}} \quad [\text{m}]$$

Oinas and Sikanen (2000) provide the following H to DBH relationship for pine:

$$H = 1.3 + \exp\left(3.59 - \frac{24.67}{DBH + 5} - \frac{1.67}{(DBH + 5)^2}\right) \quad [\text{m}]$$

The total tree height H for *Pinus sylvestris* in Finland, as provided by Siipilehto (2000) using Näslund's height curve, is very similar to that provided by Cermák et al. (1998) but without having an upper tree height limit:

$$H = 1.3 + \left(\frac{DBH}{0.894 + 0.185\,DBH}\right)^2 \quad [\text{m}]$$

6.3 Height to crown, H_t [m]

The SILVA model of Pretzsch et al. (2002) makes use of the following relationship ($r^2 = 0.79$) to describe the relationship between DBH [cm] and the height to the tree crown H_t [m] - see dashed line in Figure 29):

$$H_t = H\left(1 - \exp^{(0.376 - 0.9963\frac{H}{DBH} - 0.0218\,DBH)}\right) \quad [\text{m}]$$

However, this allometric formulation makes that H_t is almost equal to the tree height H at low DBH values thus almost completely eliminating the crown length. To account for the fact that the crown of young trees often extends almost to the ground, the relationship of Cermák et al. (1998) with $r^2 = 0.62$ for a Scots pine forest with a stem density of 672 ha^{-1} is also provided

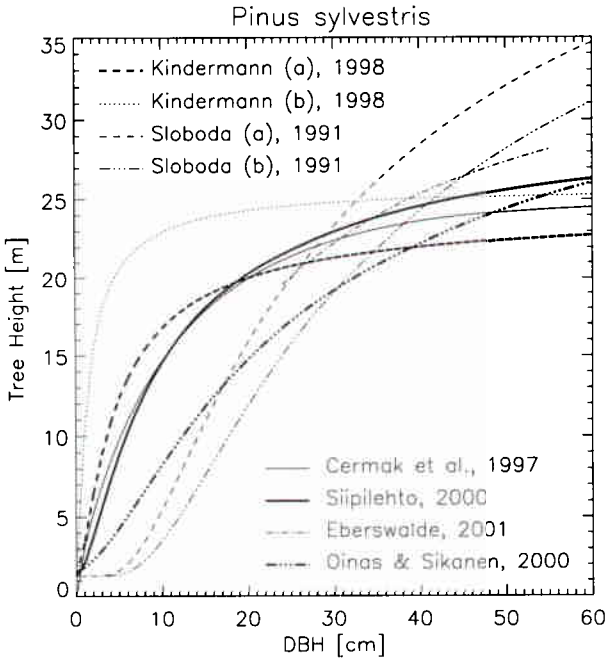

Figure 28: Tree height curves for Scots pine according to the allometric relationships of Kindermann (1998), Sloboda (1991), Cermák et al. (1997), Siipilehto (2000), Eberswalde (2001) and Oinas and Sikanen (2000).

(see solid line in Figure 29):

$$H = 16.9\left(1 - \exp^{\left(\frac{-DBH}{3.45}\right)}\right)^{9.513} \quad [\text{m}]$$

6.4 Height to the maximum crown width, H_{Cr} [m]

Pretzsch et al. (2002) indicates that the height to the maximum crown width for Scots pine can be approximated by $H_{Cr} = H_t + H_c/2$ where $H_c = H - H_t$. Thus:

$$H_{Cr} = H_t + \frac{H - H_t}{2} \quad [\text{m}]$$

6.5 Height to first dead branch, H_{nb} [m]

No direct information as to a possible parameterization of H_{nb} for Scots pine was available. Schmidt (2001) provides two empirical relationships (equations 31 and 32) to determine the height to the lowest dead branch:

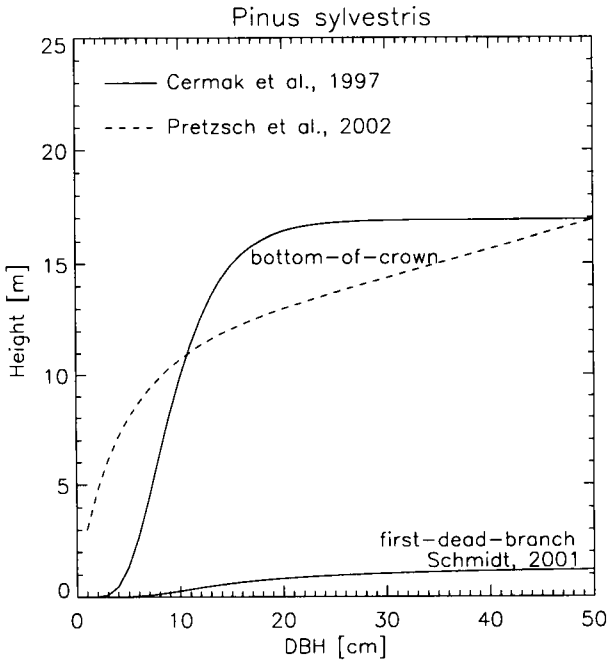

Figure 29: Allometric relationships of Cermák et al., (1997) and Pretzsch et al., (2002) for the height to the bottom of the live crown of Scots pine.

$$
\begin{aligned}
H_{nb} &= H_{gb}\left(\exp^{\frac{(b_0 H)^{b_1}}{b_2}} - 1\right) \text{ [m]} \\
H_{gb} &= H_t\left(1 - 0.39017 \exp^{-0.01202 H_t}\right) \text{ [m]}
\end{aligned}
$$

where H_{gb} is an estimate of the lowest green branch - which can be situated below what Schmidt (2001) terms the height to the bottom of the crown. In the above, however, only the equation for H_{gb} was parameterized for Scots pine. Due to a lack of data points, Schmidt (2001) could not provide any information as to the parameters for the equation giving H_{nb}. As a possible solution the values indicated for *Picea abies* ($b_0 = 0.523; b_1 = 1.7, b_2 = 1000$) are shown in Figure 29.

6.6 Maximum crown radius, C_r [m]

Equation 12 in Pretzsch et al. (2002) describes the relationship between tree height H and the maximum crown diameter ($C_D = 2\,C_r$) [m] in an exponential manner (compare with short dashed line in Figure 30). Using the parameter of their Table 8 ($r^2 = 0.79$):

$$C_r = \exp\left(-0.5515 + 0.6468 \ln\left(\frac{H}{DBH}\right) - 0.0062\,H + 0.1904 \ln(DBH)\right) \text{ [m]}$$

Nagel et al. (2002) provides another relationship between DBH and crown radius: (long dashed line in Figure 30):

$$C_r = (0.63915 + 0.05694\,DBH)\left(1 - \exp^{-\left(\frac{DBH}{8.70522}\right)^{1.33944}}\right) \text{ [m]}$$

The allometric equation of Cermák et al. (1998) (r^2=0.853) lies somewhat in between the estimates of the two equations above (thick line in Figure 30):

$$C_r = \sqrt{\left(\frac{0.0067\,DBH^2 + 0.2126\,DBH}{\pi}\right)} \quad [\mathrm{m}]$$

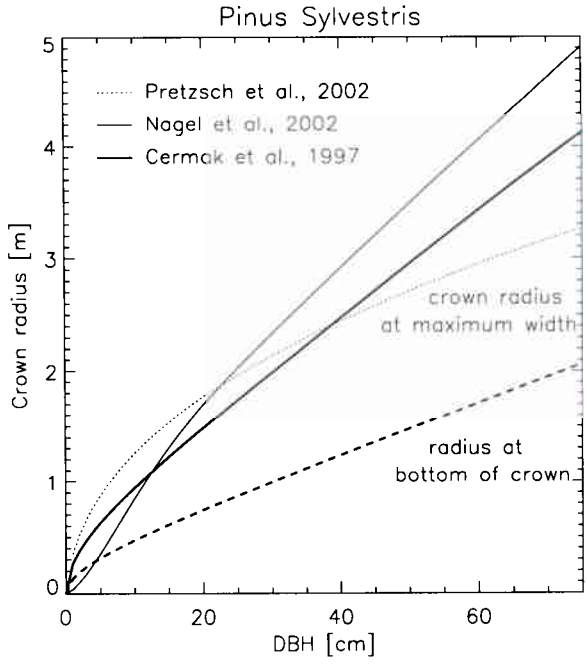

Figure 30: The allometric relationships for Scots pine of Pretzsch et al., (2002) between the DBH [cm] and the maximum crown radius C_r [m] as implemented in the SILVA model, the equivalent relationship of Nagel et al. (2002) as implemented in the BWINPro6.1 model, and the same relationship when derived by Cermák et al. (1997). Also indicated is the radius at the bottom of the live crown based on the C_r values of Cermák et al. (1997)

6.7 Bottom crown radius, R_c [m]

According to table 2.1 of Pretzsch (1992) the crown radius at the bottom of the tree crown (that is at height H_t) can be approximated with (see Figure 30):

$$R_c = C_r/2. \quad [\mathrm{m}]$$

6.8 Leaf Area Index, LAI [tree^{-1}]

Cermák et al. (1998) provides two relationships to estimate the needle area A_l [m^2 tree^{-1}] and the crown projected area C_A [m^2 tree^{-1}] on the basis of DBH [cm] measurements (between 16 and 48 cm) for a Scots pine stand in Braschaat, Belgium. The leaf area index per tree $LAI = A_l/C_A$ can thus be written (compare with solid and dashed black line in Figure 31):

$$LAI = \frac{12.607\,DBH - 5.093}{1.389\,DBH - 3.061} \quad [\mathrm{tree}^{-1}]$$

Burger (1941b) provides the following relationship for the single sided foliage area A_l:

$$A_l = \frac{1}{2}\left(1.548\,DBH + 0.078\,DBH^2\right) \quad [\mathrm{m^2\,tree^{-1}}]$$

The leaf area index values that may be derived from this measure of A_l (using the crown area of Cermák et al. (1998)) are shown in Figure 31 and do not converge to zero at small values of the DBH. The same is also true for the LAI relationship of Cermák et al. (1998), which when extrapolated yields an LAI superior to 1 as the DBH $\rightarrow$ 0. An empirical relationship has been fitted to the valid range of the latter data to force the LAI to tend towards zero as the DBH $\rightarrow$ 0 (compare with thick grey line in Figure 31). The difference in LAI between this and the original curves at DBH=70 cm is roughly 0.5.

$$LAI = \exp(0.375)\,DBH^{0.375} \quad [\mathrm{tree^{-1}}]$$

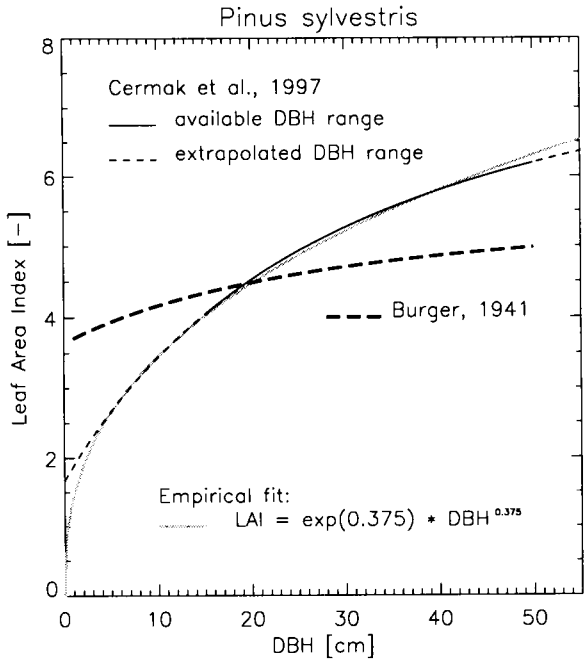

Figure 31: The Leaf Area Index (LAI) for Scots pine when derived from the allometric relationships for 'leaf area per tree' and 'crown projection area per tree' of Cermák et al. (1997): The black solid line indicates the range of available DBH data from which the relationship was derived, the thin dashed lines are extrapolated values. The thick grey line is an empirical fit to the DBH-LAI relationship of Cermák et al., that forces the LAI to vanish in the limit as the DBH $\rightarrow$ 0 cm. Also shown is the ratio of Burger's leaf area estimate and the projected crown area using C_r of Cermák et al. (thick dashed line).

6.9 Foliage and Biomass

According to Stenberg et al. (1994) the needles of *Pinus sylvestris* achieve a length of 5–7 cm in favourable conditions. Their retention time is between 3 and 6 years, being longer in the higher latitudes. The mean specific needle area (all sides) is $\sim$ 14 $\mathrm{m^2/kg}$ but variations are large (although Nilson et al. (1999) indicates also a value of 7.52 $\mathrm{m^2/kg}$ for the (one sided) specific needle area). Stenberg et al. (1994) indicates that the vertical distribution of foliar biomass is

skewed towards the upper half of the tree height (compare with section 7.3).

Cermák et al. (1998) provides a relationship to estimate the dry mass of the needles per tree W_f [kg $tree^{-1}$] on the basis of DBH [cm] measurements for a Scots pine stand in Braschaat, Belgium ($r^2 = 0.956$):

$$W_f = -0.0003\,DBH^2 + 0.0433\,DBH - 0.4908 \quad [\mathrm{kg\,tree^{-1}}]$$

Mencuccini and Grace (1994) provide the following allometric relationships for the needle dry mass (W_f) of two stands in the north ($r^2 = 0.72$) and south ($r^2 = 0.69$) of the United Kingdom:

$$W_f = 0.0943\,DBH^2 - 0.950 \quad [\mathrm{kg\,tree^{-1}}]$$
$$W_f = 0.0628\,DBH^2 - 0.380 \quad [\mathrm{kg\,tree^{-1}}]$$

Marklund (1988) provides a series of biomass estimates for Scots pine although that report is written in Swedish. Lehtonen and Vayred (2002) compare the total above ground dry weight for Scots pine in Finland (using the biomass equations of Marklund (1988)) and Catalonia, Spain. Their data can be expressed by the following (empirical) relationships:

$$W_t = 0.0943\,DBH^2 - 0.950 \quad [\mathrm{kg\,tree^{-1}}]$$
$$W_t = 0.0628\,DBH^2 - 0.380 \quad [\mathrm{kg\,tree^{-1}}]$$

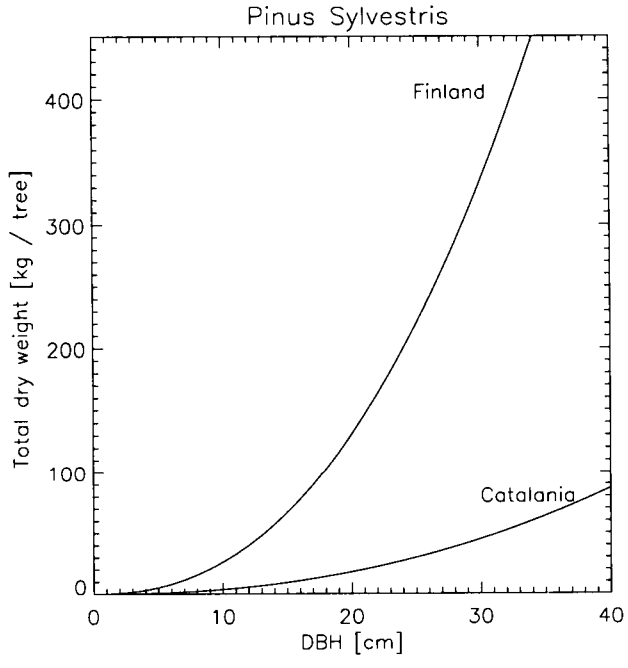

Figure 32: Total aboveground dry weight relationship for Scots pine as described by Lehtonen and Vayreda, (2002) for Scots pine in Finland and Catalonia.

General Properties of Forest Canopies

The second part of this document will describe several issues regarding structural properties of forest canopies and/or individual trees, for which not enough information was available for individual species.

7 General Properties of Forest Canopies

In this section an overview will be provided regarding 1) the shape, orientation and distribution of leaves and needles in the tree crown, 2) the spatial distribution of individual trees, the height distribution and maximum stem densities in forests, 3) inter-species competition and mixing patterns, and 4) the fractions of dead wood in forests.

7.1 The shape of leaves and needles

For the purpose of modelling the radiation transfer within forest canopies it is not sufficient to describe the tree structure, without accounting for the size (and shape) of these primary scattering elements themselves. They play an important role in defining the hot spot effect—a strong increase in the observed reflectance value when the view direction falls exactly along the illumination direction, due to the absence of shadows within the field of view of the observer in that case. In most radiation transfer models, foliage elements are simulated as flat disc-like entities of a particular size, the spatial locations of which are either described in a deterministic manner, or else statistically accounted for within certain predefined volumes (*i.e.*, within the crown, or, within the shoot).

Figure 33: Top row from left to right: The shoots of *Pinus sylvestris*, *Picea abies* and *Larix decidua*. Bottom row from left to right: A pair of leaves from *Fagus sylvatica* and *Betula pendula*. Photographs by Anna-Lena Anderberg, (Source: `http://linnaeus.nrm.se/flora/`).

Figure 33 presents the shape of typical leaves (bottom row) and needles (top row) for the tree species described in this report. To a good approximation most leaf-shapes (despite being irregular in their outline) agree sufficiently well with the disc-like scatterer assumption often

encountered in radiation transfer models. Needles, however, are of a very different nature. First they are rarely flat in their cross-sections, and second, they possess no clearly distinctive upper and lower sides. Furthermore needles tend to be clumped into shoots, which themselves occur along branches attached to individual whorls. Such features may impose a different approach to characterising the properties of needles (*e.g.*, the one sided leaf area index), and/or may require the definition of new observational protocols.

7.2 The orientation of foliage in crowns

Leaf orientation is of importance since, together with leaf shape and size, it accounts for the intercepted fraction of solar radiation and thus affects photosynthesis. The proper statistical description of leaf orientation is a complex issue due to extreme variety of vegetation forms in space and time as well as across plant species. For example, in conifers the needles are clumped into shoots, which themselves appear to be oriented in an azimuthally independent manner (Stenberg et al. 1994). Other plants, like the sunflowers for example, are known to change their orientations in response to solar illumination.

Nevertheless, a series of mathematical expressions have been formulated that—although simplifications of reality—allow for the description of a wide range of existing leaf angle distributions. These statistical distributions assume a large number of foliage elements whose spatial orientation is described by the direction of their normal $\mathbf{\Omega}_L(\theta_L, \phi_L)$ to the upper surface, where θ_L is the zenith angle of the leaf normal, and ϕ_L is the azimuth angle of the outward normal. The leaf-normal distribution (LND) function $g_L(z, \mathbf{\Omega}_L)$, then denotes the fraction of total leaf area in the horizontal layer of unit thickness at height z whose normals fall within a unit solid angle around the direction $\mathbf{\Omega}_L$, and must satisfy the following normalization criterion (Ross 1981):

$$\frac{1}{2\pi} \oint_{2\pi+} g_L(\mathbf{\Omega}_L)\, d\mathbf{\Omega}_L \;=\; \frac{1}{2\pi} \int_0^{2\pi} d\phi_L \int_0^{\pi/2} g_L(\theta_L, \phi_L) \sin\theta_L \, d\theta_L \;\equiv\; 1$$

Although two-dimensional LND's have been treated in theoretical studies (Strebel et al. 1985, Verstraete 1987) observations (*e.g.*, Oker-Blom and Smolander 1988, Stenberg et al. 1994) have shown that for a significant number of species the foliage or shoot orientation is to a large degree azimuthally independent. Such an assumption significantly reduces the mathematical complexity of the function $g_L(\theta_L, \phi_L)$. Out of the various models to describe azimuthally independent leaf normal distribution functions ($g_L^*(\theta_L) = g_L(\theta_L) \sin\theta_L$), the two most commonly used are 1) the trigonometric functions of Bunnik (1978):

$$g_L^*(\theta_L) \;=\; (\, a + b\cos 2\theta_L + c\cos 4\theta_L \,) \tag{8}$$

and 2) the beta functions of (Goel and Strebel 1984):

$$g_L^*(\theta_L) \;=\; \frac{2}{\pi} \frac{x^{\xi-1}(1-x)^{\nu-1}}{B(\xi,\nu)} \qquad\qquad 0 < x < 1 \tag{9}$$

where $B(\xi,\nu) = \Gamma(\xi)\Gamma(\nu)/\Gamma(\xi+\nu)$ is the beta function, Γ is the gamma function and $x = 2\theta_L/\pi$.

In Table 1 the parameters for the above two representations of $g_L^*(\theta_L)$ are given for a variety of leaf normal distributions. Note however, that the descriptive term given to the LNDs refers to g_L^* rather than g_L. This is most notably seen in what are termed *uniform* and *spherical* leaf normal distributions, namely:

$g_L(\theta_L)$	$= \frac{2}{\pi}(\sin\theta_L)^{-1}$	$g_L^*(\theta_L)$	$= \frac{2}{\pi}$	uniform
$g_L(\theta_L)$	$= 1$	$g_L^*(\theta_L)$	$= \sin\theta_L$	spherical

Table 1: Parameter values for the trigonometrical (a, b, c) and beta (ξ, ν) function representation of the probability density function, $g_L^*(\theta_L)$ for 6 different leaf-normal distributions.

	uniform	**spherical**	**planophile**	**erectophile**	**plagiophile**	**extremophile**
a	$2/\pi$	$\sin\theta_L$	$2/\pi$	$2/\pi$	$2/\pi$	$2/\pi$
b	0	0	$2/\pi$	$-2/\pi$	0	0
c	0	0	0	0	$-2/\pi$	$2/\pi$
ξ	1.000	1.101 (1.066)†	2.770 (2.531)	1.172 (1.096)	3.326	0.433
ν	1.000	1.930 (1.853)	1.172 (1.096)	2.770 (2.531)	3.326	0.433

†The values used by Govaerts (1996) are shown in brackets if different from Goel and Strebel (1984).

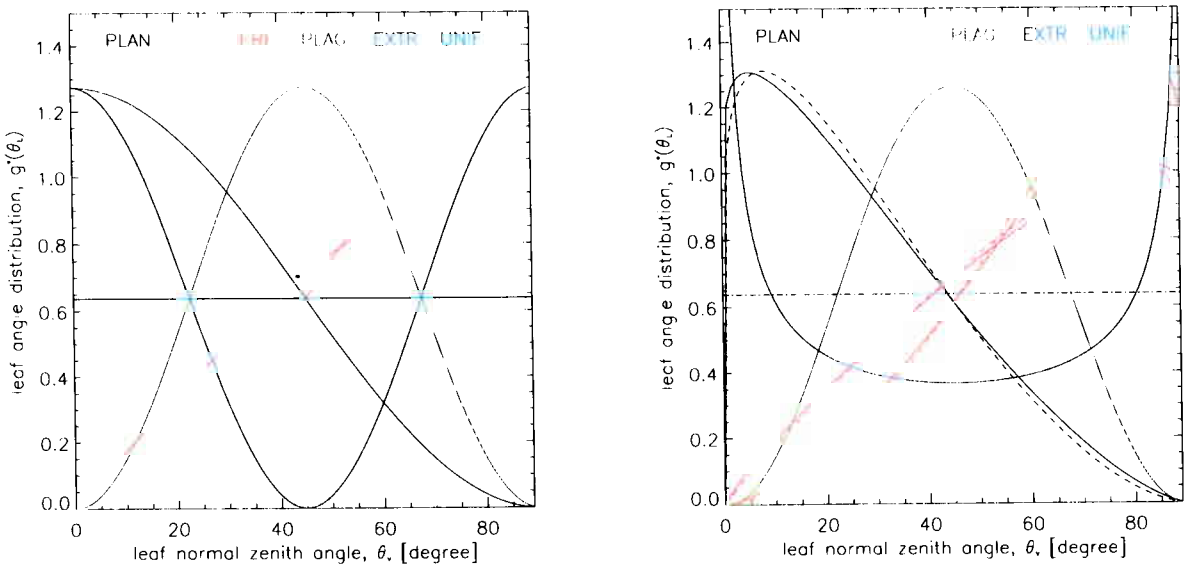

Figure 34: Left panel: The function $g_L^*(\mathbf{\Omega})_L$ for the azimuthally independent leaf normal distribution $\mathbf{\Omega}_L$ according to Bunnik's formulation. Right panel: The function $g_L^*(\mathbf{\Omega})_L$ for the azimuthally independent leaf normal distribution $\mathbf{\Omega}_L$ according to Goel's (dashed) and Govaert's (solid) formulation.

Erectophile and planophile leaf normal distributions are known to occur in nature. For example, clover is essentially planophile, whereas most grasses, as well as Eucalyptus and Weeping Willow foliage on the other hand are erectophile. (Hagemeier 2002) states that, in the lower shadowed part of the crown, the leaf angle deviations from the horizontal are 20^o for beech, 15^o for lime and 19^o for oak, whereas pioneer trees like the birch have leaf angle deviations from the horizontal that lie around 42^o. However, within the crowns of individual trees different leaf normal distributions may occur at different heights as was shown by (Stenberg et al. 1994) for the shoot zenith angle distribution in Scots pine stands.

7.3 The distribution of foliage in crowns

The distribution of foliage is not random within tree crowns. Many empirical studies have been performed to determine the one or two dimensional distributions of foliage within tree crowns, *e.g.*, Stenberg et al. (1994), Kinerson and Fritschen (1970), Wang et al. (1990). Cermák et al. (1998) report an upward skewed foliage area distribution in Scots pine, Massman (1982) spec-

ified that the maximum foliage amount is often located at about 80 % of the tree height for old-growth coniferous tree canopies. Webb and Ungs (1992) even provide information on the three-dimensional distribution patterns of needle surface area in a single Douglas fir tree. Overall, it can be stated that a single peak in the vertical leaf area density distribution is common amongst many vegetation canopies *e.g.*, Ross (1981).

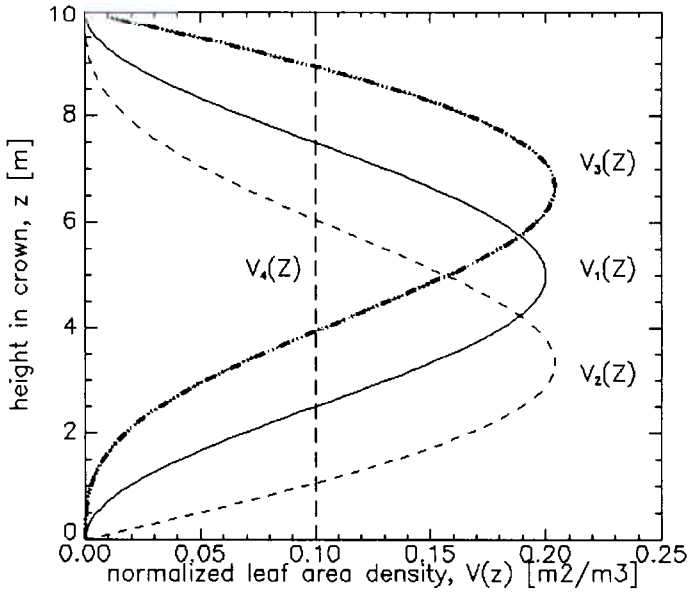

Figure 35: Four examples for the vertical distribution of the normalized leaf area density in a tree crown of $H_c = 10$ m vertical extent - according to Chen (1994). Note that the integral of the normalized leaf area density over H_c is unity.

Chen et al. (1994) provide a series of equations to describe the vertical variations of the normalized leaf area density $V(z)$, where z is some height above the bottom of the tree crown ($z = 0$ at H_t) and below the top of the crown (H). Thus $0 < z < H - H_t = H_c$ and the leaf area index of any particular height interval $\Delta z = z_2 - z_1$ of a tree having a total leaf area index of LAI can be calculated as:

$$LAI_{\Delta z} = \int_{z_1}^{z_2} V(z)\, LAI\, dz \qquad [\mathrm{m}^2/\mathrm{m}^2]$$

Four different vertical profiles are provided by Chen et al. (1994): $V_1(z)$ - which peaks in the lower part of the canopy, $V_2(z)$ - which has the highest foliage density in the middle part of the crown, $V_3(z)$ - having its peak in the upper part of the crown, and $V_4(z)$ - which is constant throughout the vertical extent of the tree crown:

$$\begin{aligned}
V_1(z) &= \frac{1}{H_c}\left[1 - \cos\left(\frac{2\pi z}{H_c}\right)\right] && [\mathrm{m}^2/\mathrm{m}^3] \\
V_2(z) &= \frac{\pi}{2H_c}\left[\sin\left(\frac{2\pi z}{H_c}\right) + \frac{1}{2}\sin\left(\frac{\pi z}{H_c}\right)\right] && [\mathrm{m}^2/\mathrm{m}^3] \\
V_3(z) &= \frac{\pi}{2H_c}\left[\sin\left(\frac{2\pi z}{H_c}\right) - \frac{1}{2}\sin\left(\frac{\pi z}{H_c}\right)\right] && [\mathrm{m}^2/\mathrm{m}^3] \\
V_4(z) &= \frac{1}{H_c} && [\mathrm{m}^2/\mathrm{m}^3]
\end{aligned}$$

Both Massman (1982) and Cermák et al. (1998) report on an upward skewed leaf area distribution for conifers that is not unlike the one described by $V_3(z)$.

7.4 The foliage-free interior of crowns

When trees grow their leaf area is generally increasing as well. Since the outer regions of a tree crown tend to receive more light than their inner counterparts (*i.e.*, those that are closer to the tree trunk), foliage growth occurs predominantly on the fringes of the crown. This process will however reduce the light availability along the central axis of the crown, which will lead to the development of foliage free volumes within the crown. The larger the size of a tree, the more shadowing of the inner crown volume will occur, and hence the greater the foliage-free volume within the crown Mayer (1980). Only qualitative evidence of this process was found in the literature. Figure 36 is an adaptation from works of Badoux (1952), Burger (1927), and Assman (1961).

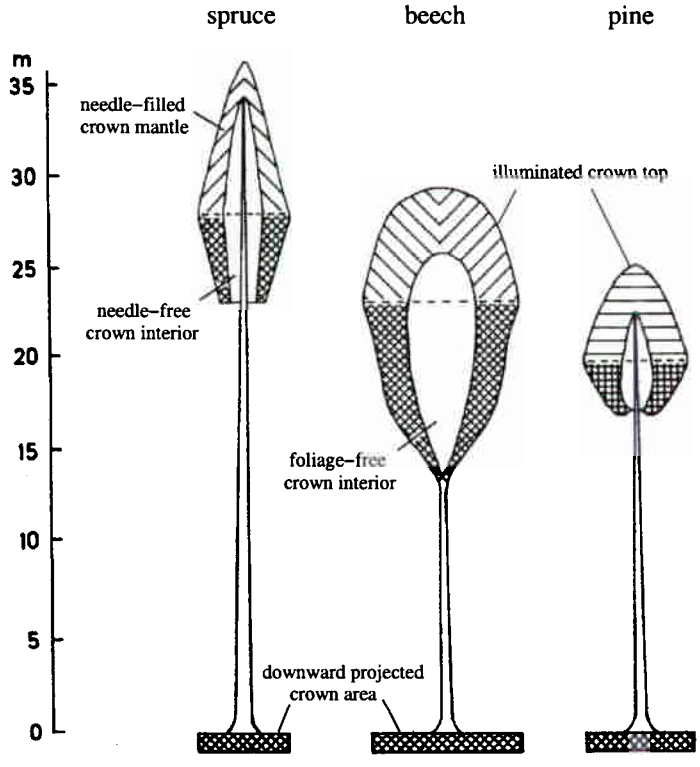

Figure 36: The vertical extent of the foliage-free crown volume for 90 year old spruce, beech and pine trees – adapted from the works of Badoux (1952), Burger (1927) and Assman (1961).

One can see from Figure 36 that the vertical extent of the foliage free crown volume depends on tree species (as well as on tree age and stand density among others). In the absence of further quantitative information, it is suggested here to utilize the vertical profiles of subsection 7.3, to delineate the vertical variations in the foliage-free crown volume.

7.5 The spatial distribution of tree locations

Frelich et al. (1993) propose three factors that influence forest patterns: 1) the disturbance history , 2) competitive interactions, and 3) invaders. The published results on tree distributions

in unmanaged forests have shown a predominance of random patterns (Szwagrzyk 1990, Tomppo 1986). The findings of Franklin et al. (1985), Moeur (1993) and Kenkel (1983) suggest that clustering patterns are not common to most forests: smaller trees tend to exhibit more random features while larger trees show more uniform or regular patterns. However, the density of the stand and the scale of investigation are two major variables affecting the statistical conclusion on the spatial organisation of trees (Cressie 1993). 3-D radiation transfer simulations of forest stands, that are to be used in LUT-based inversion schemes, thus simulate the spatial distribution of the trees with a simple Poisson model regardless of the stand densities (Wu and Strahler 1994, Franklin et al. 1985). Case studies might however require the generation of various degrees of tree-clustering. One such example was taken from Coops and Culvenor (2000) and is presented in Figure 37.

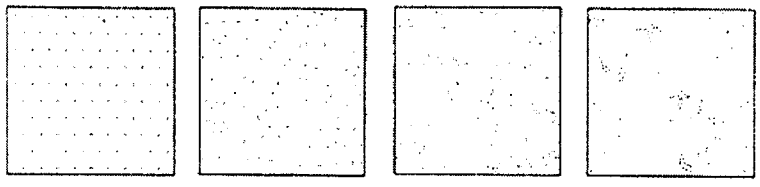

Figure 37: Regular organisation of point patterns (left panel), as well as various types of spatial patterns from random (second from left) to more and more clustered (second from right and rightmost panel) as generated by Coops and Culvenor (2000).

7.6 The height distribution of trees

Although tree height distributions are often assumed to behave log-normal (Hafley and Scheuner 1977), tree height, age and DBH are interlinked in relatively complex manner depending on species and forest site. The first two of these variables are often linked to each other through the Chapman-Richards equation:

$$H_{pot} = A(1 - \exp^{-kt})^p \quad [\text{m}]$$

where H_{pot} is the potential tree height at age t, and A, k and p are species-specific parameters, which are derived from a vector of site variables. Tree height can then be related to DBH via a series of allometric equations like those described in the first part of this document.

An alternative approach is to derive the DBH distribution for individual species and then to relate this directly to the tree heights in the stand. Nagel and Biging (1995) describe the distribution of DBH values for individual species using a Weibull function with two parameters that depend on 1) the diameter-at-breast-height value of the tree with the average basal area in the stand, D_g [cm], 2) the maximum DBH value in the stand, D_{max} [cm] and, 3) the downward projected total area of the stand, G [m^2/ha].

7.7 The maximum tree density in forests

Maximum tree density numbers result from the natural size of tree crowns as well as their requirements for light availability. According to Reineke (1933), in even-aged 'full-density' stands the relationship between the quadratic mean diameter-at-breast-height, D, and their number per unit, N is linear on a log-log scale:

$$\log(N) = a - b \log(DBH)$$

where a and b are species specific parameters. Zeide (1995) provides an additional term (c) to this equation, claiming that it improves the accuracy of the prediction:

$$\log(N) = a - (b + cH) \log(DBH)$$

Pretzsch et al. (2002) give the following equation for the maximum tree density of *Picea Abies*:

$$\log(N) = -1.75 \log(D_g) + 19.63$$

where D_g is the diameter-at-breast-height of the tree in the stand having the average basal area. Figure 38 shows the evolution of trunk density as a function of tree age as provided by Mayer (1980).

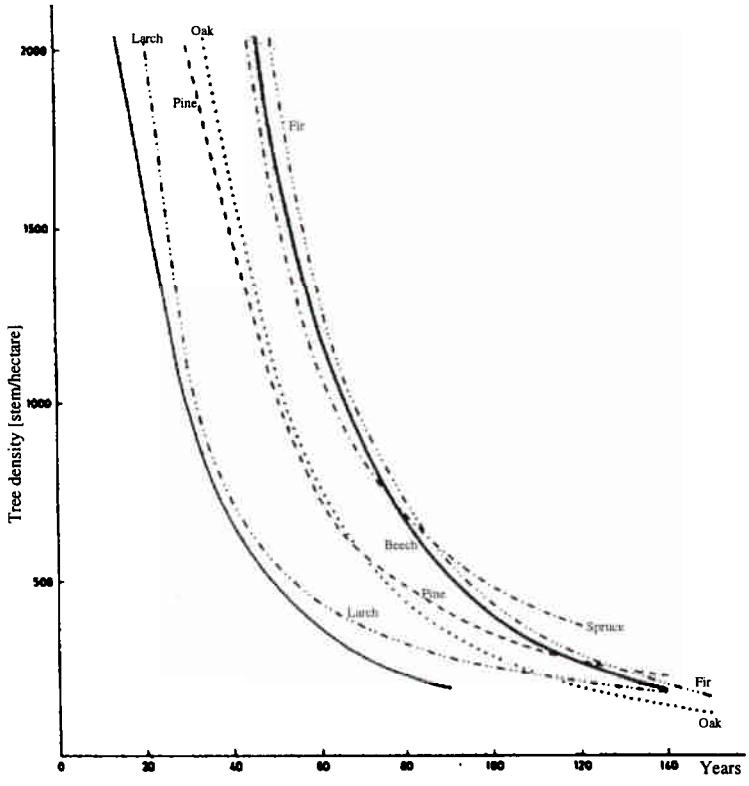

Figure 38: The number of trees as a function of age for a series of European tree species as provided by Mayer (1980)

7.8 The fraction of dead wood in forests

Ferguson and Archibald (2002) find that tree mortality is relatively constant across forest age. They find a 3/4 power law between live and dead tree basal area. The percentage of stems that were dead was greatest in young forest (18% of stems in 0-60-year-old forests), decreased to a low percentage of 12% in 61-80-year-old forests, and thereafter increased with age of forests from 15% to 16% in 81-100, > 100 year-old forests. Nilsson et al. (2002) state that amongst old-growth trees in Europe, 1) about 10% of all standing trunks are dead and 2) about 30% of the basal area and volume of dead trees are standing (snags). However, the distribution of the dead wood amongst standing stems with and without crown, and lying stems is species-dependent. For example, Spelsberg (2000) indicates that amongst the total dead wood for beech (oak) in western Germany 25% (64%) are standing with crown, 27% (25%) are standing but without crown, and 48% (19%) are lying. Overall they claim that the fraction of dead wood is about 1% of that of living wood.

7.9 Mixed forests, tree competition and mortality

The stand density and crown closure of a forest is a compromise between two opposing processes: lateral growth of the branches and roots which increases closure, and mortality of trees (by whatever cause) which diminishes it. As trees become older and larger, the size of a gap created by a fallen tree increases, while the ability of neighbouring trees to close the gap decreases. Soil properties, light and water availability, and local weather conditions affect the development of individual trees. To simulate the evolution of forests over time—with or without disturbances—a series of dynamical models have been developped. Whilst these models go beyond the scope of this document, the interested reader is invited to investigate the references below: Nagel et al. (2002), Botkin (1993), Pacala et al. (1993), Pretzsch et al. (2002), Bugmann (1994).

Table 2: List of mathematical symbols, their meaning and units.

Variable	Meaning	Units
A_l	leaf area of crown	$m^2\,tree^{-1}$
A_r	vertically downward projected crown area	m^2
AGB	above ground biomass	$kg\,ha^{-1}$
C_D	maximum crown diameter	m
C_r	maximum crown radius	m
d	downward distance from top of the tree crown	m
DBH	diameter at breast height (137 cm above ground)	cm
DBH_{max}	maximum occurring diameter at breast height	cm
D	quadratic mean DBH in stand	cm
D_g	DBH value of tree with average basal area in stand	cm
D_{max}	maximum DBH value in the stand	cm
G	downward projected total area of the stand	$m^2\,ha^{-1}$
$g_L(z,\Omega_L)$	leaf normal distribution function	–
H	tree height	m
H_{max}	maximum occurring tree height	m
H_c	vertical dimension of the crown	m
H_{cb}	vertical dimension of the bottom part of the crown	m
H_{Cr}	height from ground to the maximum lateral crown dimension	m
H_{ct}	vertical dimension of the top part of the crown	m
H_{db}	height from first dead branch to onset of (lower) crown	m
H_{nb}	height from ground to the first dead branch	m
H_{pot}	potential height of a tree at age t	m
H_t	height to the crown	m
$LAI_{\Delta z}$	leaf Area Index within height interval Δz	$m^2\,m^{-2}$
LAI_{max}	maximum occurring leaf area index per tree	$m^2\,m^{-2}\,tree^{-1}$
LAI	leaf Area Index per tree	$m^2\,m^{-2}\,tree^{-1}$
N	tree number per unit area	m^{-2}
PLA	projected leaf area	m^2
R_c	crown radius at lower end (bottom) of crown	m
r_b	crown radius within bottom part of the crown	m
r_t	crown radius within top part of the crown	m
SLA_p	specific leaf area	$m^2\,kg^{-1}$
t	tree age in years	year
t_d	day in year	–
$V(z)$	normalized leaf area index	$m^2\,m^{-3}$
W_b	dry weight of branches per tree	$kg\,tree^{-1}$
W_c	dry weight of crown (branches + foliage) per tree	$kg\,tree^{-1}$
W_f	dry weight of foliage per tree	$kg\,tree^{-1}$
W_s	dry weight of stem (trunk) per tree	$kg\,tree^{-1}$
W_t	total dry weight of tree	$kg\,tree^{-1}$
z	height within the canopy	m
Δz	height interval within canopy/crown	m
θ_L	zenith angle of the leaf normal	rad
ϕ_L	azimuth angle of the leaf normal	rad
$\Omega_L(\theta_L,\phi_L)$	direction of the leaf normal	rad

References

Assman, E. (1961). *Waldertragskunde.* München - Bonn - Wien: BLV Verlag.

Badoux, E. (1952). Notes sur la production du mélèze. Mitteilungen der S.A.F.V. 28, Schweizerische Anstalt für das Forstliche Versuchswesen, Züricherstrasse 111, CH-8903 Birmensdorf, SLF Davos, Switzerland.

Bartelink, H. H. (1997). Allometric relationships for biomass and leaf area of beech (Fagus Sylvatica L.). *Annales des Sciences Forestières 54*, 39–50.

Botkin, D. B. (1993). *Forest Dynamics: An ecological model.* New York: Oxford University Press.

Bragg, D. C. (2001). A local basal area adjustment for crown width prediction. *Northern Journal of Applied Forestry 18*, 22–28.

Bugmann, H. K. M. (1994). On the ecology of mountainous forests in a changing climate: A simulation study. PhD Dissertation 10638, Swiss Federal Institute of Technology Zürich, Zürich, Switzerland.

Bunnik, N. J. J. (1978). The multispectral reflectance of shortwave radiation of agricultural crops in relation with their morphological and optical properties. Technical report, Mededelingen Landbouwhogeschool, Wageningen, The Netherlands.

Burger, H. (1927). Die Lebensdauer der Fichtennadeln. Mitteilungen der S.A.F.V. 78, Schweizerische Anstalt für das Forstliche Versuchswesen, Züricherstrasse 111, CH-8903 Birmensdorf, SLF Davos, Switzerland.

Burger, H. (1941a). Holz Blattmenge und Zuwachs: V Fichten und Föhren verschiedener Herkunft auf verschiedenen Kulturorten. Mitteilungen der S.A.F.V. 22, Schweizerische Anstalt für das Forstliche Versuchswesen, Züricherstrasse 111, CH-8903 Birmensdorf, SLF Davos, Switzerland.

Burger, H. (1941b). Holz Blattmenge und Zuwachs: VI Ein Plenterwlad mittlerer Standortsgüte. Mitteilungen der S.A.F.V. 22, Schweizerische Anstalt für das Forstliche Versuchswesen, Züricherstrasse 111, CH-8903 Birmensdorf, SLF Davos, Switzerland.

Burger, H. (1945). Holz Blattmenge und Zuwachs: V Die Lärche. Mitteilungen der S.A.F.V. 24, Schweizerische Anstalt für das Forstliche Versuchswesen, Züricherstrasse 111, CH-8903 Birmensdorf, SLF Davos, Switzerland.

Burger, H. (1949). Holz Blattmenge und Zuwachs: V Die Buche. Mitteilungen der S.A.F.V. 26, Schweizerische Anstalt für das Forstliche Versuchswesen, Züricherstrasse 111, CH-8903 Birmensdorf, SLF Davos, Switzerland.

Cermák, J., F. Riguzzi, and R. Ceulemanns (1998). Scaling up from individual tree to the stand level in Scots pine. I. Needle distribution, overall crown and root geometry. *Annales des Sciences Forestières 55*, 63–88.

Cescatti, A. (1997). Modelling the radiative transfer in discontinuous canopies of assymetric crowns. I. Model structure and algorithms. *Ecological Modelling 101*, 263–274.

Chen, J. M., P. M. Rich, S. T. Gower, J. M. Norman, and S. Plummer (1997). Leaf area index of boreal forests: Theory, techniques and measurements. *Journal of Geophysical Research 102*, 29,429–29,443.

Chen, S. G., B. Y. Shao, I. Impens, and R. Ceulemans (1994). Effects of plant canopy structure on light interception and photosynthesis. *Journal of Quantitative Spectroscopy and Radiation Transfer 52*, 115–123.

Comeau, P., J. Wang, T. Letchford, and D. Coopersmith (1999). Effects of spacing paper birch-mixedwood stands in central British Columbia FRBC project HQ96423-RE (MOF EP 1193). Extension Note 29, British Columbia Ministry of Forest Research Program.

Coops, N. and D. Culvenor (2000). Utilizing local variance of simulated high spatial resolution imagery to predict spatial pattern of forest structure. *Remote Sensing of Environment 71*, 248–260.

Cressie, N. A. (1993). *Statistics for spatial data.* New York: John Wiley and Sons.

De Reffye, P. and F. Houllier (1997). Modelling plant growth and architecture: Some recent advances and applications to agronomy and forestry. *Current Science 73*, 984–992.

Diner, D. J., J. C. Beckert, T. H. Reilly, C. J. Bruegge, J. E. Conel, R. A. Kahn, J. V. Martonchik, T. P. Ackerman, R. Davies, S. A. W. Gerstl, H. R. Gordon, J.-P. Muller, R. B. Myneni, P. J. Sellers, B. Pinty, and M. M. Verstraete (1998). Multi-angle imaging spectroradiometer MISR instrument description and overview. *IEEE Transactions on Geoscience and Remote Sensing 36*, 1072–1087.

Dohrenbusch, A., R. Grote, and H. W. Fritz (1993). Struktur und Wachstum eines Fichtenbestandes unter experimenteller Manipulation des Stoffeinträge. *Forstarchiv 64*, 172–177.

Eberswalde, L. (2001). *Adam Schwappach - ein Forstwissenschaftler und sein Erbe.* 29582 Hanstedt, Germany: Nimrod Verlag.

Ferguson, S. H. and D. J. Archibald (2002). The 3/4 power law in forest management: How to grow dead trees. *Forest Ecology and Management 169*, 283–292.

Forstreuter, M (1999). Ergebnisbericht: Ökologie der Gehölze i. Report SS99, Institut für Ökologie und Biologie, Technische Universität Berlin, Königin-Luise-Str. 22, Berlin 14195.

Franklin, J., J. Michaelsen, and A. H. Strahler (1985). Spatial analysis of density pattern in coniferous forest stands. *Vegetatio 64*, 29–36.

Frelich, L. E., R. L. Calcote, M. B. Davis, and J. Pastor (1993). Patch formation and maintenance in an old-growth hemlock-hardwood forest. *Ecology 72*, 513–527.

Goel, N. S., L. B. Knox, and J. M. Norman (1991). From artificial life to real life: Computer simulation of plant growth. *International Journal of General Systems 18*, 291–319.

Goel, N. S. and D. E. Strebel (1984). Simple beta distribution representation of leaf orientation in vegetation canopies. *Agronomy Journal 76*, 800–803.

Govaerts, Y. (1996). A model of light scattering in three-dimensional plant canopies: A Monte Carlo ray tracing approach. EUR Report No. 16394 EN, Space Applications Institute.

Govaerts, Y., O. Engelsen, B. Pinty, and M. M. Verstraete (1997). Identification of a particular tropical forest environment on the basis of simulated NOAA-AVHRR reflectance factors. In *Proceedings of the 7th ISPRS International Symposium on Physical Measurements and Signatures in Remote Sensing, Courchevel, France, 7–11 April 1997*, pp. 727–734. Balkema/Rotterdam/Brookfield.

Govaerts, Y. and M. M. Verstraete (1998). Raytran: A Monte Carlo ray tracing model to compute light scattering in three-dimensional heterogeneous media. *IEEE Transactions on Geoscience and Remote Sensing 36*, 493–505.

Gower, T. S., C. J. Kucharik, and J. M. Norman (1999). Direct and indirect estimation of leaf area index, FAPAR, and net primary production of terrestrial ecosystems. *Remote Sensing of Environment 70*, 29–51.

Gower, T. S., P. B. Reich, and Y. Son (1993). Canopy dynamics and aboveground production of five tree species with different leaf longevities. *Tree Physiology 12*, 327–345.

Grote, R. (1999). Foliage and branch biomass estimation of coniferous and deciduous tree species. *Silva Fennica 36*, 779–788.

Guericke, M. (2001). Growth dynamics of mixed stands of beech and European larch. Technical report, Fakultät für Forstwissenschaften und Waldökologie, Georg-August-Universität, Göttingen, Germany.

Hafley, W. I. and H. T. Scheuner (1977). Statistical distributions for fitting diameter and height data in even aged stands. *Canadian Journal of Forest Research 7*, 481–489.

Hagemeier, M. (2002). *A functional study of the treetop architecture of Central European silver birch, scots pine, sessile oak, little leaf linden and European beech.* Berlin, Stuttgart, Germany: Dissertationes Botanicae, Band 361, Gebr. Borntraeger.

Halliwell, D. H. and Apps, M. J. (1997). BOReal Ecosystem-Atmosphere Study (BOREAS) biometry and auxiliary sites: overstory and understory data. Report Version 3.03, Canadian Forest Service, Northern Forest Centre, 5320 122 Street, Edmonton, Alberta, Canada.

Heräjärvi, H. (2001). Technical properties of mature birch (Betula pendula and B. pubescens) for saw milling in Finland. *Silva Fennica 35*, 469–485.

Jenkins, J. C., D. C. Chojnacky, L. S. Heath, and R. A. Birdsey (2003). National-scale biomass estimators for United-States tree species. *Forest Science 49*, 12–35.

Johansson, T. (1999). Biomass production of Norway Spruce (Picea abies (L.) Karst.) growing on abandoned farmland. *Silva Fennica 33*, 261–280.

Joosten, R. and A. Lehtonen (2002). Comparison of biomass expansion factors between conifer and broadleaf species in temperate and boreal forests. First results of a biomass study in the German state North Rhine-Westphalia and a joint project university of applied science Lippe and Höxter and METLA (Helsinki). In *COST E21 workshop, 7-8 October 2002, Valencia, Spain*, pp. 5. `http://www.bib.fsagx.ac.be/coste21/report/2002-10-07.html`.

Kajimoto, T., Y. Matsuura, M. A. Sofrono, A. V. Volokitina, S. Mori, A. Osawa, and A. P. Abaimov (1999). Above- and below ground biomass and net primary productivity of a *Larix gmelinii* stand near Tura, central Siberia. *Tree Physiology 19*, 815–822.

Kenkel, N. C. (1983). Pattern of self-thinning in Jack pine: Testing the random mortality hypothesis. *Ecology 69*, 1017–1024.

Kerner, H., E. Gross, and W. Koch (1977). Structure of the assimilation system of a dominating spruce tree (Picea abies (L.) Karst.) of closed stands: Computation of needle surface area by means of variable geometric needle model. *Flora 166*, 449–459.

Kindermann, G. E. (1998). Die Flächenanteile der Baumarten. Diplomarbeit, Institut für Waldwachstumsforschung, Universität für Bodenkultur, Perchtoldsdorf, Deutschland.

Kinerson, R. J. and L. J. Fritschen (1970). Modelling a coniferous forest. *Agricultural Meteorology 8*, 439–445.

Knape, C. (1996). Waldbauliche Behandlung von Birkenbeständen auf R- und K-Standorten in Mecklenburg-Vorpommern. Dissertation, Technische Universität Dresden, 01735 Tharandt, Germany.

Knyazikhin, Y., J. V. Martonchik, D. J. Diner, R. B. Myneni, M. M. Verstraete, B. Pinty, and N. Gobron (1998). Estimation of vegetation canopy leaf area index and fraction of absorbed photosynthetically active radiation from atmosphere-corrected MISR data. *Journal of Geophysical Research 103*, 32,239–32,256.

Kramer, H. (1982). Kurzfristige Zuwachsreaktionen bei Buche in Abhängigkeit von Witterung und verschiedenen Baummerkmalen. *Allgemeine Forst und Jagdzeitung 153*, 57–67.

Kranigk, J., F. Gruber, J. Heimann, and A. Thorwest (1994). Ein Modell für die Kronenraumstruktur und die räumliche Verteilung der Nadeloberfläche in einem Fichtenbestand. *Allgemeine Forst und Jagd Zeitung 165, Jg. 10-11*, 193–197.

Küssner, R. and R. Mosandl (2000). Comparison of direct and indirect estimation of leaf area index in mature Norway spruce stands of eastern Germany. *Canadian Journal of Forest Research 30*, 440–447.

Lehtonen, A. and J. Vayred (2002). Biomass expansion factors for Scots pine (*Pinus sylvestris*), comparison between Catalonia and Finland. In *COST E21, WG-1 workshop on biomass, 4-5 July 2002, Besalú, Spain*, pp. 5. `http://www.bib.fsagx.ac.be/coste21/report/2002-07-04.html`.

Lischke, H., T. J. Loeffler, and A. Fischlin (1998). Aggregation of individual trees and patches in forest succession models: Capturing variability with height structures, random, spatial distributions. *Theoretical Population Biology 54*, 213–226.

Marklund, L. G. (1988). Biomass functions for pine, spruce and birch in Sweden. Report 45, Swedish University of Agricultural Sciences, Department of Forest Survey, Umeå.

Martin, J. G., B. D. Kloeppel, T. L. Schaefer, D. L. Kimbler, and S. G. McNulty (1998). Aboveground biomass and nitrogen allocation of ten deciduous southern Appalachian tree species. *Canadian Journal of Forest Research 28*, 1648–1659.

Massman, J. W. (1982). Foliage distribution in old-growth coniferous tree canopies. *Canadian Journal of Forest Research 12*, 10–17.

Mayer, H. (1980). *Waldbau*. Stuttgart, New York: Gustav Fischer Verlag.

Mencuccini, M. and J. Grace (1994). Climate influences the leaf area/sapwood area ratio in Scots pine. *Tree Physiology 15*, 1–10.

Moeur, M. (1993). Characterizing spatial patterns of trees using stem-mapped data. *Forest Science 39*, 756–775.

Muusche, S., R. Samson, L. Nachtergale, A. De Schrijver, R. Lemeur, and N. Lust (2001). A comparison of optical and direct methods for monitoring the seasonal dynamics of leaf area index in deciduous forests. *Silva Fennica 35*, 373–384.

Myneni, R. B., R. R. Nemani, and S. W. Running (1997). Estimation of global leaf area index and absorbed PAR using radiative transfer models. *IEEE Transactions on Geoscience and Remote Sensing 35*, 1380–1393.

Nagel, J., M. Albert, and M. Schmidt (2002). Das waldbauliche Prognose- und Entscheidungsmodell BWINPro 6.1. *Forst und Holz 57*, 486–493.

Nagel, J. and G. S. Biging (1995). Schätzung der Parameter der Weibullfunktion zur Generierung von Durchmesserverteilungen. *Allgemeine Forst und Jagd Zeitung 166*, 185–189.

Nihlgård, B. (1972). Plant biomass, primary production and distribution of chemical elements in a beech and planted spruce forest in southern Sweden. *OIKOS 23*, 69–81.

Nilson, T., J. Anniste, M. Lang, and J. Praks (1999). Determination of needle area indices of coniferous forest canopies in the NOPEX region by ground based optical measurements and satellite images. *Agricultural and Forest Meteorology 98-99*, 449–462.

Nilsson, S. G., M. Niklasson, J. Hedin, G. Aronsson, J. M. Gutowski, P. Linder, H. Ljungberg, G. Mikusiński, and T. Ranius (2002). Densities of large living and dead trees in old-growth temperate and boreal forests. *Forest Ecology and Management 161*, 189–204.

North, P. R. J. (1996). Three-dimensional forest light interaction model using a Monte Carlo method. *IEEE Transactions on Geoscience and Remote Sensing 34*, 946–956.

Oinas, S. and L. Sikanen (2000). Discrete event simulation model for purchasing of marked stands, timber harvesting and transportation. *Forestry 73*, 283–301.

Oker-Blom, P. and H. Smolander (1988). The ratio of shoot silhouette area to total needle area in Scots Pine. *Forest Science 34*, 894–906.

Pacala, S. W., C. D. Canham, and J. A. J. Silander (1993). Forest models defined by field measurements: I The design of the northeastern forest simulator. *Canadian Journal of Forest Research 23*, 1980–1988.

Pacala, S. W., C. D. Canham, J. A. J. Silander, R. K. Kobe, and E. Ribbens (1996). Forest models defined by field measurements: Estimation, error analysis and dynamics. *Ecological Monographs 66*, 1–43.

Pinty, B., J.-L. Widlowski, N. Gobron, and M. M. Verstraete (2002). Uniqueness of multi-angular information - Part 1: A surface heterogeneity indicator from MISR. *IEEE Transactions on Geoscience and Remote Sensing 40*, 1560–1573.

Pretzsch, H. (1992). Konzeption und Konstruktion von Wuchsmodellen für Rein- und Mischbestände. Forstliche Forschungsberichte München 115, Schriftenreihe der Forstwissenschaftlichen Fakultät der Universität München und der Bayerischen Forstlichen Versuchs- und Forschungsanstalt.

Pretzsch, H., P. Biber, and J. Durský (2002). The single tree-based stand simulator SILVA: construction, application and evaluation. *Forest Ecology and Management 162*, 3–21.

Prskawetz, M. and M. J. Lexer (2000). Evaluierung des LI-COR LAI-2000 zur Ermittlung des Blattflächenindex in Buchenjungbeständen. *Allgemeine Forst und Jagdzeitung 171*, 185–191.

Reineke, L. H. (1933). Perfecting a stand-density index for even-aged forests. *Journal of Agricultural Research 46*, 627–638.

Röhrig, E. (1980). *Waldbau auf öologischer Grundlage. Der Wald als Vegetationstyp und seine Bedeutung für den Menschen.* Hamburg and Belrin, Germany: Paul Parey.

Röser, C., R. Montagnani, E. Detlef-Schulze, D. Mollicone, O. Kolle, M. Meroni, D. Papale, L. B. Marchesini, S. Federici, and R. Valentini (2002). Net CO2-exchange rates in three different successional stage of 'Dark Taiga' of Central Siberia. *Tellus 54*, 642–659.

Ross, J. (1981). *The Radiation Regime and Architecture of Plant Stands.* Boston: W. Junk.

Scharf, E. (2001). Das Wachstum der Baumart Sandbirke (*Betula pendula* ROTH) in ausgewählten Beständen der Sächsischen Forstämter Colditz und Strassgräbchen. Dissertation, Thüringer Fachhochschule für Forstwirtschaft, Schwarzburg, Germany.

Scherzer, J., F. Suckow, J. Müller, M. Wegehenkel, M. Lukes, K. Hammel, A. Kniess, and M. Meesenburg (2003). Wasserhaushalt von Waldökosystemen: Methodenleitfaden zur Bestimmung der Wasserhaushaltskomponenten auf Level II-Flächen. Level ii ag wasserhaushalt, Bundesministerium für Ernährung, Landwirtschaft und Forsten, Rochusstrae 1, 53123 Bonn.

Schmidt, M. (2001). Models for predicting wood quality criteria of important tree species. Technical report, Fakultät für Forstwissenschaften und Waldökologie, Georg-August-Universität, Göttingen, Germany.

Schmidt-Vogt, H. (1976). Fichtenherkünfte der Bundesrepublik Deutschland. Erste Auswertung der Versuchsreihe 1959/66. *Allgemeine Forst und Jagdzeitung 147*, 149–163.

Shao, G. (1986). Kopide: A computer model of forest growth and succession on Changbai mountain. Ph.d. dissertation, Chinese Academy of Sciences.

Siipilehto, J. (2000). A comparison of two parameter prediction methods for stand structure in Finland. *Silva Fennica 34 (4)*, 331–349.

Sloboda, B. (1991). Untersuchungen zur Erstellung eines regionalen und bestandesindividuellen Sortenmodells für die Pfälzer Kiefer. Sachbericht zum Forschungsprojekt AZ D/0228/7211/Je, Abteilung für forstliche Biometrie und Informatik der Universität Göttingen, Göttingen, Germany.

Spelsberg, G. (2000). Totholz im Nordrhein-Westfälischen Wald. Bericht über den ökologischen Zustand des Waldes, Ministerium für Umwelt und Naturschutz, Landwirtschaft und Verbraucherschutz, LÖBF Recklinghausen.

Stenberg, P., T. Kuuluvainen, T. Kellomaeki, J. C. Grace, E. J. Jokela, and H. L. Gholz (1994). Crown structure, light interception and productivity of pine trees and stands. In H. L. Gholz, R. McMurthie, and S. Linder (Eds.), *A comparative analysis of pine forest productivity*, pp. 20–43. Copenhagen: Ecological Bulletins (43).

Strebel, D. E., N. S. Goel, and K. J. Ranson (1985). Two-dimensional leaf orientation distributions. *IEEE Transactions on Geoscience and Remote Sensing 23*, 640–647.

Szwagrzyk, J. (1990). Small-scale spatial patterns of trees in a mixed Pinus sylvestris-Fagus sylvatica forest. *Forest Ecology and Management 51*, 301–315.

Thompson, R. L. and N. S. Goel (1998). Two models for rapidly calculating bidirectional reflectance: Photon spread (ps) model and statistical photon spread (sps) model. *Remote Sensing Reviews 16*, 157–207.

Tiangxiang, L., R. P. Neilson, C. J. Vörösmarty, H. Zua, and S. Liu (2002). A model for seasonality and distribution of leaf area index of forests and its application to China. *Journal of Vegetation Science 13*, 817–830.

Tomppo, E. (1986). Models and methods for analyzing spatial patterns of trees. *Communicationes Instituti Forestais Fenniae 138*, 65.

Tomppo, E. (2000). Remote sensing requirements to support forest inventories. In M. M. Verstraete, M. Menenti, and J. Peltoniemi (Eds.), *Observing Land from Space: Science, Customers and Technology*, pp. 151–160. Dordrecht, Boston, London: Kluwer Academic Publishers.

Van Deusen, P. C. and G. S. Bigin (1985). STAG - A stand generator for mixed species stands. Research Note 11, Northern California Forest Yield Cooperative, Department of Forestry and Rescource Management, University of California, Berkeley, USA.

Verstraete, M. M. (1987). Radiation transfer in plant canopies: Transmission of direct solar radiation and the role of leaf orientation. *Journal of Geophysical Research 92*, 10,985–10,995.

Viherä-Aarnio, A. and P. Velling (1999). Growth and stem quality of mature birches in a combined species progeny trial. *Silva Fennica 33*, 225–234.

von Droste zu Hülshoff, B. F. (1969). Struktur und Biomasse eines Fichtenbestandes auf Grund einer Dimensionsanalyse an oberirdischen Baumorganen. Dissertation, Staatswirtschaftliche Fakultät der Ludwig-Maximillians-Universität München, Munich, Germany.

Wang, J. R. and J. P. Kimmins (2002). Height growth and competitive relationship between paper birch and Douglas fir in coast and interior of British Columbia. *Forest Ecology and Management 165*, 285–293.

Wang, Y. P., P. G. Jarvis, and M. L. Benson (1990). Two-dimensional needle-area density distribution within the crowns of *Pinus radiata*. *Forest Ecology and Management 32*, 217–237.

Webb, W. and M. J. Ungs (1992). Three-dimensional distribution of needle and stem surface area in a Douglas fir. *Tree Physiology 13*, 203–212.

Webster, R. C. and C. G. Lorimer (2003). Comparative growing space efficiency of four tree species in mixed conifer-hardwood forests. *Forest Ecology and Management 177*, 361–377.

Widlowski, J.-L., B. Pinty, N. Gobron, and M. M. Verstraete (2001). Detection and characterization of boreal coniferous forests from remote sensing data. *Journal of Geophysical Research 106*, 33,405–33,419.

Wu, Y. and A. H. Strahler (1994). Remote estimate of crown size, stand density and biomass on the Oregon transect. *Ecological Applications 4*, 299–312.

Zeide, B. (1995). A relationship between size of trees and their number. *Forest Ecology and Management 72*, 265–272.

Mission of the JRC

The mission of the JRC is to provide customer-driven scientific and technical support for the conception, development, implementation and monitoring of EU policies. As a service of the European Commission, the JRC functions as a reference centre of science and technology for the Union. Close to the policy-making process, it serves the common interest of the Member States, while being independent of special interests, whether private or national.

EUROPEAN COMMISSION
DIRECTORATE-GENERAL
Joint Research Centre